Dental Materials 40 (2024) 1097–1112

Contents lists available at ScienceDirect

Dental Materials

journal homepage: www.elsevier.com/locate/dental

Water absorption in artificial composites: Curse or blessing?

Thomas Niem *, Antje Hübner, Bernd Wöstmann

Department of Prosthodontics, Justus-Liebig University, Schlangenzahl 14, 35392 Giessen, Germany

ARTICLE INFO

Keywords:
CAD/CAM composite materials
Water sorption
Hydrolytic degradation
Equilibrium state
Loss tangent
Damping properties

ABSTRACT

Objectives: This study evaluated the impact of mutable water uptake on the durability of mechanical properties and the long-term reliability of artificial composites.
Methods: Three resin-based CAD/CAM restorative materials (CRMs) were investigated in three-point bending tests to calculate flexural strength (FS), modulus of elasticity (ME), modulus of resilience (MR), modulus of toughness (MT), and elastic recovery (ER). All specimens (n = 180) were stored under the same conditions and tested in four subsets (n = 15 per material) that were respectively withdrawn after repeated thermocycling (5000 cycles; 5–55 °C, H_2O) and repetitive drying (7 d; 37 °C, air). For every specimen, weight differences were determined per storage condition. Likewise, loss tangent data were separately recorded via dynamic mechanical analysis to reliably assess damping characteristics.
Results: Repeated thermocycling always induced weight increase and a concurrent significant loss in all mechanical properties except for MT and ER of a polymethylmethacrylate-based CRM. Drying consistently provoked weight loss and raised mechanical properties to initial values. Weight increase, however, enhanced loss tangent values and accordingly distinct damping characteristics, whereas weight decrease markedly lowered damping properties.
Significance: Water uptake repeatedly induced a decrease in common mechanical properties but concurrently increased damping behavior. Invertible equilibrium processes were found with no evidence for permanent material degradation.

1. Introduction

Guaranteeing the clinical functionality of artificial biomedical restorative materials requires the preservation of their material properties during useful life. Besides a multitude of endogenous and exogenous variables that influence the behavior of materials in a particular way, a key factor that still merits careful observation is the ubiquitous uptake of solvents, especially water. This phenomenon, present in many artificial restorative materials, still plays an increasing role in dentistry as, besides the influence on material swelling and plasticizing [1], the effect of water is more frequently associated with permanent and irreversible destruction and persistent mechanical degradation processes [2–5]. Therefore, examining the long-term influences of such adverse hygroscopic and hydrolytic effects appears to be particularly important for estimating clinical success during a material's useful life. Water-based stability issues observed for dental restorative materials containing polymerized resin structures are frequently discussed for filling materials [4,6] as well as bonding [7–9] and luting [10] systems. However, it is not clear whether the effects observed can be assigned to reversible processes of equilibrium states.

In general, the impact of water uptake in artificial composite-based materials can be categorized into effects emerging in the pure resin/polymer structures [11–13], the embedded fillers [14,15], and the interface between fillers and resin structures [3, 16–18], namely the adhesion-promoting silane coating usually applied to the filler surface via a vulnerable silanization process [19–22]. This interlayer is frequently associated with hydrolytic material failure [3, 18, 23–25]. However, Plueddemann et al. [26] described equilibrium processes in this layer and Sideridou et al. [27] an advantageous effect of such systems on the dynamic mechanical properties (loss tangent = tan δ) of dental composites that were ultimately very beneficial for generating energy dissipation effects and hence providing long-term material stability. Likewise, Ye et al. [28] reported related sol-gel equilibria in the wet environment providing 'intrinsic reinforcement of the polymer network', 'improved hydrolytic stability', and 'enhanced mechanical properties'. Such simple water equilibrium systems are widespread in

* Corresponding author.
E-mail address: thomas.niem@dentist.med.uni-giessen.de (T. Niem).

https://doi.org/10.1016/j.dental.2024.05.018
Received 18 December 2023; Received in revised form 22 March 2024; Accepted 13 May 2024
Available online 28 May 2024

many biological composite materials, and in the wet condition, they provide pronounced energy dissipation capabilities and hence excellent long-term stability [29]. Most of these natural damping effects are practically realized via well-known energy consumption mechanisms like sacrificial bonds and hidden lengths [30,31]. In these particular cases, and in general, the presence of water appears to be vitally important for equilibrium formation [32] and therefore has a tremendous effect on the genesis of long-term material stability [33]. Likewise, bone [34] and tooth [35] structures were shown to reveal a markedly improved stability when investigated in the moist state compared to examinations conducted under dry conditions [36].

Nevertheless, many in vitro tests originally invented to optimally simulate clinical situations with the aim of obtaining deeper insights into the long-term behavior of artificial restorative materials in a moist environment still use processes with varied water storage conditions and different timescales at ambient, low or elevated temperatures (e.g. non-standardized thermocycling procedures [37]). Unfortunately, such investigations are performed without considering relevant time-dependent equilibrium processes, such as mutable water sorption [38–40] and viscoelastic material behavior [41,42], even though both effects are usually present at the same time in most polymer-based restorative materials. Consequently, the acquired datasets, which often show a reduction in relevant material properties, possibly lack decisive time-dependent information and thus, incorrect interpretations may be made, especially misleading material comparisons. Hence, in this context, caution should be exercised in using the common technical term 'hydrolytic degradation' in the original sense of deleterious effects resulting from permanent and irreversible processes after water uptake when describing final study results. It should be primarily reserved for transformation processes of biopolymers where a conscious chain scission of chemical structures is intended to generate a special effect or function, such as in medical therapies [43,44].

Adverse hygroscopic and hydrolytic effects in dental as well as other biomedical restorative materials typically emerge via the alteration of mechanical properties and especially via their substantial decline. It is not yet clear whether these are generally provoked by irreversible chemical degradation processes or are associated with reversible processes of equilibrium states as well, which means they might even enhance material stability in a moist environment by degrading rigidity and brittleness. Therefore, this in vitro study set out to examine the influence of mutable water sorption on selected mechanical properties of three different resin-containing CAD/CAM restorative materials. Ceramic materials were not included in this investigation as our previous studies showed no detectable deleterious effect of the water content on common mechanical properties [45]. The aim was to determine the flexural strength (FS), modulus of elasticity (ME), modulus of resilience (MR), modulus of toughness (MT), and elastic recovery (ER), together with separately measured loss tangent data (tan δ), received via dynamic mechanical analysis (DMA), to further characterize damping properties and viscoelastic deformation effects. The rationale and detailed description of MR, MT, and ER data have been previously reported [46].

Two null hypotheses were tested: 1) There is no association between the sign of the weight differences between two different storage conditions and the storage condition itself. 2) The mechanical properties of CAD/CAM restorative materials are independent of (A) the sign of the weight difference for specimens between two different storage conditions, and (B) the material.

2. Materials and methods

2.1. Materials

For this comparative study, three commonly used CRMs were selected from two different material types, namely composites and polymers, which both exhibit deviant filler contents (Table 1).

Table 1
Tested materials.

Material type	Brand	Code	Manufacturer	Lot No.[$]	Filler content / %[#]
Composite	Lava Ultimate A2 HT	LU	3M ESPE	N430105 (b)	72.0
	Shofu Block HC A2 LT	SB	SHOFU Inc.	021501 (b)	61.8
Polymer	M-PM Disc A2	MPM	Merz Dental GmbH	10417 (d)	0.1

[$] b, block; d, disc.
[#] Ashing in air (1 h, 700 ± 20 °C, n = 3) [47,48].

2.2. Specimen preparation

2.2.1. Three-point bending

Due to limited milling block dimensions and to enable reliable comparisons, bar-shaped specimens (4.0 x 1.5 x 17.0 mm^3 ± 0.1 mm^3, n = 60) were prepared for each investigated material in accordance with ISO 6872 [49] using a water-cooled precision saw (IsoMet™1000, Buehler, Esslingen, Germany) in combination with a diamond-coated saw blade (127-mm diameter, No. 11–4255, Buehler). Milling block mounts were cut off, and blocks or discs were sliced and cut to the desired dimensions. Specimen sizes were adjusted, and final surfaces were polished by grinding on wet SiC paper using P1200, P2500 (Leco Corp, Michigan, USA), and P4000 (Struers A/S, Ballerup, Denmark) successively. All materials were used under ambient laboratory conditions (23 ± 1 °C; 50 ± 5% relative humidity) [50] according to the manufacturer's instructions.

2.2.2. Dynamic Mechanical Analysis (DMA)

Bar-shaped specimens (4.00 x 1.00 x 16.00 mm^3 ± 0.05 mm^3, n = 9) were prepared for each investigated CRM. The procedure of cutting and polishing was exactly the same as described in Section 2.2.1. Special care was taken during the adjustment of the specimen thickness to attain perfectly plano-parallel surfaces within the required specification throughout the entire bar.

2.3. Storage conditions and data acquisition

2.3.1. Three-point bending

The workflow of the weighing and mechanical properties testing procedure is described in detail in Fig. 1 A. Directly after preparation, all specimens (n = 60) were separately labeled on the head side for each CRM using a pencil, placed on a filter paper without any further treatment, and stored for 14 days under strictly controlled ambient laboratory conditions (23 ± 1 °C; 50 ± 5% relative humidity). This allowed the formation of a balanced equilibrium state and avoided adverse physicochemical changes in the material structure that possibly arise from uncontrolled desiccation processes. Subsequently, each specimen was separately weighed with a newly calibrated analytical balance (XS205 Dual Range, Mettler Toledo, Giessen, Germany; accuracy: ± 0.01 mg) to determine the baseline of dry weight w_{ax} (x = 0 for the beginning) before the first controlled water absorption took place. Next, the first cycle of the thermocycling process was initiated using all 60 specimens at once. Each thermocycling process was conducted with 5000 cycles in 5 - 55 °C distilled water baths (Thermocycler THE 1100, SD Mechatronik, Feldkirchen-Westernham, Germany). Each cycle lasted 120 s: 45 s in a 5 °C bath, 15 s to drain and transfer the samples to the second bath, 45 s in a 55 °C bath, and 15 s to transfer the samples back to the 5 °C bath. After completion, all specimens were carefully taken out one by one using tweezers, dried on filter paper until free from visible moisture (23 ± 1 °C; 50 ± 5% relative humidity), waved in the air for 10 s, and

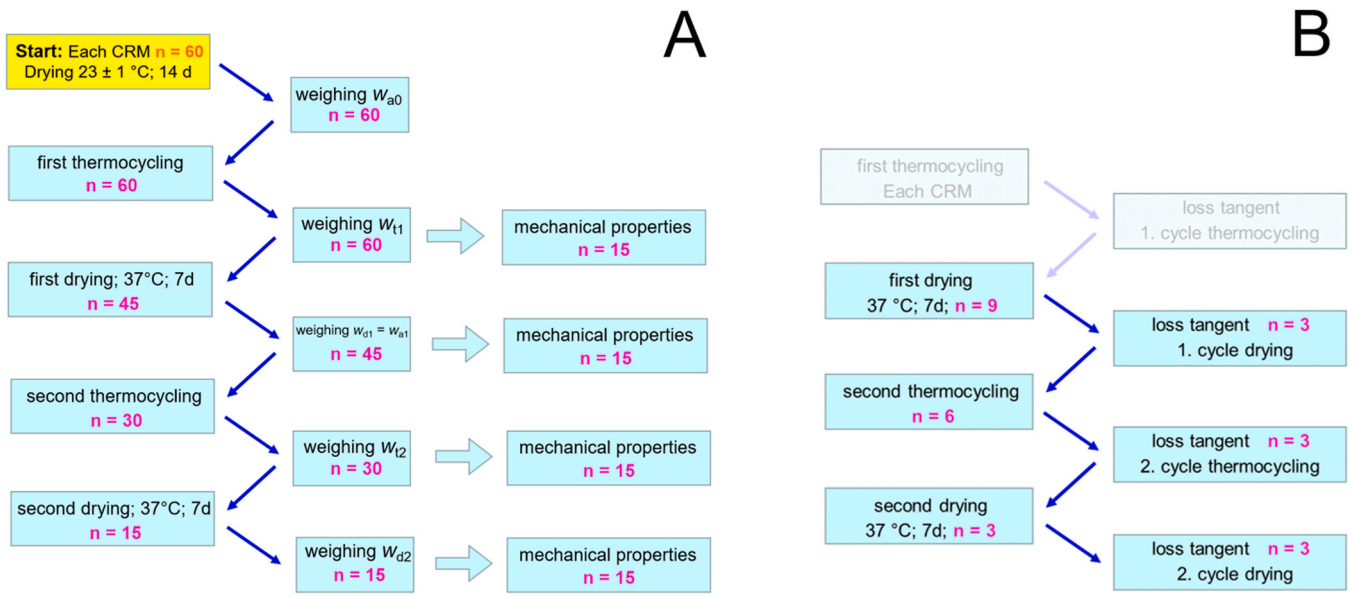

Fig. 1. Workflow describing storage conditions and their different weighing cycles A) for mechanical property determination and B) for loss tangent determination. Frosted and faint parts of the figure denote skipped process steps.

immediately weighed to ± 0.01 mg to obtain the weight after the first thermocycling w_{tx} (x = 1 for the first cycle). Immediately after each weighing, 15 specimens were partly withdrawn one by one and subjected to a three-point bending test.

All remaining specimens of the same CRM (n = 45) were transferred into an incubator (Ehret, Emmendingen, Germany), placed on a filter paper (lateral surface) and dried at 37 °C for 7 d. Subsequently, all specimens were cooled down to reach ambient laboratory conditions (23 ± 1 °C; 50 ± 5% relative humidity) and weighed in succession as described above to obtain the weight for each specimen after the first drying process w_{dx} (x = 1 for the first cycle). This was identical to the starting value for the weight of the second cycle w_{ax} (x = 1; $w_{d1} = w_{a1}$). Again, after each weighing, a total of 15 specimens were withdrawn one by one and subjected to a three-point bending test while all residual specimens (n = 30) were again subjected to thermocycling and subsequent drying as described above to generate further weight datasets (w_{tx} and w_{dx}; x = 2) for the second process cycle. At each weighing step, 15 specimens were again withdrawn one by one to determine the respective mechanical properties for the second cycle.

The procedure described above was conducted in the same way for each separate CRM. The total number of 60 specimens finally led to 5 different datasets comprising weight data before/after thermocycling and before/after drying (Fig. 1A, second row). At the same time, 4 datasets were obtained for the mechanical properties that consisted of results acquired after each thermocycling and drying step (Fig. 1A, third row).

2.3.2. Dynamic Mechanical Analysis (DMA)

Exactly the same storage conditions were applied as described in Section 2.3.1 to separately determine loss tangent data for each CRM by using specimens with thinner dimensions (see Section 2.2.2). No additional weighing of each specimen was performed such as described for the three-point bending test, and so de novo water absorption and desorption were not assessed. The entire investigation was started for each CRM by subjecting all specimens (n = 9) to the 'first cycle of drying' (37 °C; 7 d) and thus skipping the first thermocycling process. Fig. 1B shows the workflow. Three specimens were removed to investigate loss tangent values (tan δ) after the first cycle of material drying. For the remaining specimens (n = 6) the second cycle of thermocycling was initiated as described in Section 2.3.1, followed by the removal of three specimens after completion of the treatment to again determine loss tangent data (2. Cycle thermocycling). The remaining three specimens were then dried once more as described above (37 °C; 7 d) and used to finally measure loss tangent (2. Cycle drying).

The procedure described above was performed in the same way for each separate CRM where the total amount of 9 specimens per CRM finally led to three different datasets comprising loss tangent data for one thermocycling and two drying cycles (Fig. 1B). Only these three storage types were investigated, consciously skipping the first cycle of thermocycling. This guaranteed reliable dry starting conditions by taking into account a potentially different inherent water content of each investigated CRM immediately after it was purchased because the storage conditions prior to purchase were not known.

2.4. Calculation of water absorption and water desorption

The water absorption and desorption properties of all CRM specimens were expressed as percentage increase or decrease of weight, respectively, after thermocycling and drying for a predetermined time (see Section 2.3). This was done by using the following equations for weight differences after absorption (WD_A) in % (1) [51] and weight difference after desorption (WD_D) in % (2) [52]:

$$WD_A = \frac{W_{tx} - W_{ax}}{W_{ax}} \times 100 \quad (1)$$

$$WD_D = \frac{W_{dx} - W_{tx}}{W_{tx}} \times 100 \quad (2)$$

with w_{tx} (weight of the specimen after thermocycling) in g, w_{ax} (weight of dried specimen before thermocycling) in g, and w_{dx} (weight of dried specimen after thermocycling) in g all separately determined with x = 1 for the first cycle and x = 2 for the second cycle (Fig. 1A).

2.5. Three-point bending test and calculations

Specimens were loaded until rupture in a three-point bending test using a newly calibrated universal testing machine (1454, Zwick/Roell, Ulm, Germany) with a 0.5 kN load cell to minimize the effect of system compliance [53]. Specimen deflection was detected via the crosshead motion of the testing machine as previously described [54] (incremental linear encoder; repeatability f_w: 0.006 μm), and likewise, engineering stress-strain curves were used for all parameter calculations without

correction for true stress-strain material behavior. The span width (L) was 15.0 mm and the crosshead speed 1 mm/min.

Flexural strength **(FS)** in MPa [50], modulus of elasticity **(ME)** in MPa [50], and modulus of toughness **(MT)** in MJ/m^3 [46] were calculated using Eqs. (3), (4), and (5):

$$FS = \frac{3F_{max}L}{2wh^2} \tag{3}$$

$$ME = \frac{F_{lin}L^3}{4d_{lin}wh^3} \tag{4}$$

$$MT = \frac{9A}{whL} \tag{5}$$

where F_{max} (N) is the maximum load, L (mm) is the span width between the two support bars, and w (mm) and h (mm) are the width and height of the specimen, respectively. F_{lin} (N) is the force in the stress-strain curve's linear part, and d_{lin} (mm) is the corresponding deflection at F_{lin}. A (J) is the total area under the load-deformation curve (work performed by the applied load to deflect and fracture the specimen) obtained with the software (TestXpert; release 10.11, Zwick/Roell, Ulm, Germany) used for the testing machine.

(MR) [46] in MJ/m^3 (Eq. (6)) and **(ER)** [46] in MJ/m^3 (Eq. (7)) were obtained and calculated with the software used for the testing machine (TestXpert; release 10.11, Zwick/Roell, Ulm, Germany) based on the respective stress-strain diagrams:

$$MR = \frac{YS^2}{2ME} \tag{6}$$

$$ER = \frac{FS^2}{2ME} \tag{7}$$

where YS (MPa) represents the yield strength of the specimen, determined via the software as stress at 0.05% plastic deformation [46], and FS (MPa) is the flexural strength. ME (MPa) is equivalent to the respective modulus of elasticity.

2.6. Dynamic mechanical analysis

Loss tangent values were determined using a dynamic mechanical analyzer (DMA 1, Mettler Toledo, Giessen, Germany) in combination with an appropriate double-walled heating chamber. For the testing of dry specimens, the chamber was used in just air without any liquid medium but at an elevated temperature of 37.0 ± 0.5 °C (50 ± 5% relative humidity). For all wet specimens after the thermocycling process, it was filled with distilled water (Aqua B. Braun, Melsungen, Germany). The heating chamber was always warmed up using an external water bath (polystat cc1, Huber, Offenburg, Germany) to ensure a consistent temperature of 37.0 ± 0.5 °C inside the chamber. The chamber temperature was carefully monitored via the system-integrated sensor. All DMA measurements were performed in the 'three-point bending mode' using customized lower support bars with a support distance in the device of exactly 14.85 mm to allow a reliable and comparable investigation of specimens received from limited block dimensions. Specimens were centrically clamped between the three support bars with a constant pre-deformation of 158 ± 2 µm to ensure a permanent specimen contact during the cyclic load application of the test procedure. After mounting the specimen, the DMA instrument's specimen holder was immediately immersed into the heating chamber to avoid unintended cooling down of the specimen or drying out in case of wet measurements. The sealed system was allowed to equilibrate for at least 10 min to reach an inner temperature of 37.0 ± 0.5 °C before the measurement was started. A sinusoidal dynamic test load of 1 N was applied to each specimen with 1.5 Hz during an investigation period of 10 min. This frequency was used to resemble previously determined average chewing rates in the natural tooth environment as closely as possible (1.58 Hz [55], 1.33 Hz [56], 1.48 ± 0.18 Hz [57], 1.57 Hz [58]). In contrast to the investigation of conventional mechanical properties in this part of the study, which determined loss tangent data, only one single thermocycling cycle and two drying cycles were carried out (see Section 2.3.2). Three specimens were investigated to generate 15 loss tangent values (tan δ) per storage condition and accordingly 45 values per CRM. Data were analyzed via the system software (STARe System, Mettler Toledo, Giessen, Germany).

A detailed introduction to DMA technology and data acquisition is presented by Menard [59]. In general, loss tangent is defined as (Eq. (8)):

$$\tan\delta = \frac{E''}{E'} \tag{8}$$

where tan δ (dimensionless) is the loss tangent (damping factor describing the ratio of loss modulus and storage modulus with δ representing the phase lag between the applied stress and the resulting strain in a viscoelastic material), E'' is the loss modulus (material ability to lose/dissipate energy, representing the viscous component of a viscoelastic material), and E' is the storage modulus (material ability to store or return energy without phase difference between stress and strain, representing the elastic component of a viscoelastic material). Both moduli were determined by the DMA instrument as the response of the tested material to an oscillating loading condition. They were recorded simultaneously and tabulated in the system software.

2.7. Statistical analysis

A chi-square test of association [60] was performed to analyze the relation between 'weight differences of two different storage conditions', and the two parameters 'storage condition' and 'cycle of storage' for all specimens. In this test procedure for weight difference, a reduced dataset (nominal) to characterize only negative and positive weight difference values was used. The effect size and strength of the association was indicated via Cramer's V. All further correlations between 'weight difference' and 'mechanical properties' as well as 'loss tangent' were investigated via Pearson's correlation tests ($p < 0.05$) by grouping the data according to the respective CRM and using the respective scaled parameters.

Mean values and standard deviations of weight differences and mechanical properties were calculated, and the normality of data distribution was tested using the Kolmogorov-Smirnov and Shapiro-Wilk tests. A three-way multivariate analysis of variance (MANOVA) was performed on the calculated means to test the influence of the material, sign of the specimen weight difference, and storage cycle on all investigated mechanical properties (FS, ME, MR, MT, ER). Pillaïs Trace test was used on loss tangent to account for the inhomogeneity of variances. Only the main effects (material, sign of the specimen weight difference, storage cycle) were subsequently analyzed in detail. The dataset was split according to the respective material and each of the four weight differences, followed in each case by a series of follow-up one-way ANOVAs conducted in combination with Welch tests to account for the inhomogeneity of variances.

Post hoc comparisons were carried out to determine significant differences for each mechanical property and loss tangent values. The Bonferroni test was used in the case of homogeneity of variances and the Games-Howell test in the case of inhomogeneity of variances. All statistical analyses were carried out using IBM SPSS Statistics for Windows (version 26.0.0.0, IBM World Trade Corporation, Armonk, NY, USA) at a significance level of $\alpha = 0.05$.

3. Results

3.1. Chi-square test of association

The results of the chi-square test of association (2x2) show that there is a perfect association between 'weight difference' and 'storage condition' (χ^2 (1, $N = 450$) = 450,000, $p < 0.001$, $V = 1.0$) with a large effect size (Cramer's V). Hence, specimens revealing a negative sign of weight difference invariably belong to the group investigated after drying and those with a positive sign in the group after thermocycling (Table 2).

Conversely, no significant association was detected between 'weight difference' and 'cycle of storage' (χ^2 (1, $N = 450$) = 3.571, $p = 0.059$, $V = 0.089$) with a negligible effect size (Cramer's V). The sign of weight difference is therefore not significantly associated with the cycle of storage as displayed in the respective crosstab (Table 3).

3.2. Pearson's correlation test

Selected results of the Pearson's correlation tests performed are summarized in extracts in Table 4. This primarily focusses on reporting comparisons between weight difference and mechanical properties as well as loss tangent data and mechanical properties. Accordingly, significant and very strong 'negative' linear relationships were observed between weight difference and all mechanical properties (FS, ME, MR, MT, ER) for SB ($-0.751 \leq r \leq -0.890$, $p < 0.001$, $n = 60$) and LU ($-0.653 \leq r \leq -0.897$, $p < 0.001$, $n = 60$) while for MPM just strong 'negative' linear relationships ($-0.418 \leq r \leq -0.649$, $p < 0.001$, $n = 60$) were detected. The only exception was for MT were no significant correlation was observed ($r = 0.011$, $p = 0.934$, $n = 60$) (Table 4). Conversely, very strong 'positive' linear relationships were detected for all three independent CRMs between weight difference and loss tangent data ($0.846 \leq r \leq 0.994$, $p < 0.001$, $n = 45$) (Table 4, eighth row).

Furthermore, significant and likewise strong 'negative' linear relationships were found between loss tangent data and mechanical properties for all three CRMs ($-0.443 \leq r \leq -0.899$, $p \leq 0.002$, $n = 45$) with only one exception, namely again for MPM and its MT dataset. That revealed a negligible relationship with loss tangent ($r = 0.097$, $p = 0.528$, $n = 45$) (Table 4). (n, sample size; p, significance level; r, Pearson's correlation coefficient).

3.3. Three-way multivariate analysis of variance

Table 5 shows the results from the three-way MANOVA. As indicated by the p values, the two independent variables 'material' and 'weight difference' showed statistically significant effects ($p < 0.001$), while for the variable 'cycle', no significant effect was determined ($p = 0.222$). Considering the interactions, only a statistically significant effect was found ($p < 0.020$) for those combinations containing both independent variables 'material' and 'weight difference' together, whereas all other possible combinations showed no significant effect ($p \geq 0.05$) (Table 5). Large effect sizes [61] were only determined for the independent variables 'material' ($\eta_p^2 = 0.946$), 'weight difference' ($\eta_p^2 = 0.940$) and for their combination ($\eta_p^2 = 0.469$), while for all other variables and combinations negligible effect sizes were obtained ($\eta_p^2 < 0.064$).

Table 3
Association between sign of weight difference and cycle of storage.

			Cycle of storage		
			1. Cycle	2. Cycle	Total
Weight difference	Negative difference	Count	135	45	180
		% within weight difference	75.0%	25.0%	100.0%
	Positive difference	Count	180	90	270
		% within weight difference	66.7%	33.3%	100.0%
Total		Count	315	135	450
		% within weight difference	70.0%	30.0%	100.0%

Only the main effects were focused on and further analyzed in detail as they showed the highest differentiation in effect sizes. Tests of between-subject effects showing the influence on mechanical properties are described in separate tables for the fixed factors 'material' (Table 6), 'weight difference' (Table 7), and 'cycle' (Table 8). For the different 'materials' and both 'weight differences', the mechanical properties always showed 'highly significant' effects ($p < 0.001$) with large effect sizes ($\eta_p^2 > 0.338$), except for the combination 'weight difference' and MT where only a 'significant' effect was observed ($p = 0.004$, $\eta_p^2 = 0.050$) (Table 7). Conversely, for the fixed factor 'cycle' all mechanical properties revealed no significant effects ($p > 0.05$) with very low effect sizes ($\eta_p^2 < 0.020$) (Table 8).

3.4. One-way ANOVAs and post hoc comparisons

3.4.1. Weight differences

Statistical comparisons are documented with separate boxplot diagrams that display CRM medians of the calculated weight differences between various storage conditions (Fig. 2) and the respective medians of all determined mechanical properties (Figs. 3 – 8). Independent of the material and the cycle of the storage condition, thermocycling of the specimen always revealed positive weight differences, whereas after drying constantly negative weight differences were observed (Fig. 2). Comparisons of these weight differences always showed means that were significantly different ($p < 0.001$), independent of whether materials or storage conditions were compared (Fig. 2).

3.4.2. Mechanical properties and loss tangent

Opposite effects were clearly obtained for all investigated mechanical properties. After thermocycling nearly all cases showed significantly lower mean values than dried to desorb the material's inherent water (uppercase letters Figs. 3 - 7) ($p < 0.01$). Only one exception was observed for MPM with its MT (Fig. 6) and ER (Fig. 7) datasets, which revealed no such significant differences but instead showed results that were partly not distinguishable ($p > 0.05$).

Unlike the obvious effect of decreasing mechanical properties with positive specimen weight differences (thermocycling and water absorption), for loss tangent datasets, opposite results were obtained that

Table 2
Association between sign of weight difference and storage condition.

			Storage condition		
			Thermocycling	Drying 37 °C	Total
Weight difference	Negative difference	Count	0	180	180
		% within weight difference	0.0%	100.0%	100.0%
	Positive difference	Count	270	0	270
		% within weight difference	100.0%	0.0%	100.0%
Total		Count	270	180	450
		% within weight difference	60.0%	40.0%	100.0%

Table 4
Selected results of Pearson's correlation tests between weight difference values and mechanical properties (FS, ME, MR, MT, ER) and loss tangent.

CRM	property	FS [MPa]	ME [MPa]	MR [MJ/m^3]	MT [MJ/m^3]	ER [MJ/m^3]	Loss tangent
Shofu Block	Weight difference	r = −0.890, $p < 0.001$	r = −0.890, $p < 0.001$	r = −0.848, $p < 0.001$	r = −0.751, $p < 0.001$	r = −0.807, $p < 0.001$	r = 0.994, $p < 0.001$
	Loss tangent	r = −0.899, $p < 0.001$	r = −0.887, $p < 0.001$	r = −0.816, $p < 0.001$	r = −0.767, $p < 0.001$	r = −0.815, $p < 0.001$	———
Lava Ultimate	Weight difference	r = −0.843, $p < 0.001$	r = −0.897, $p < 0.001$	r = −0.861, $p < 0.001$	r = −0.653, $p < 0.001$	r = −0.765, $p < 0.001$	r = 0.991, $p < 0.001$
	Loss tangent	r = −0.824, $p < 0.001$	r = −0.897, $p < 0.001$	r = −0.819, $p < 0.001$	r = −0.579, $p < 0.001$	r = −0.718, $p < 0.001$	———
MPM Disc	Weight difference	r = −0.630, $p < 0.001$	r = −0.649, $p < 0.001$	r = −0.587, $p < 0.001$	r = 0.011, $p = 0.934$	r = −0.418, $p = 0.001$	r = 0.846, $p < 0.001$
	Loss tangent	r = −0.705, $p < 0.001$	r = −0.881, $p < 0.001$	r = −0.632, $p < 0.001$	r = 0.097, $p = 0.528$	r = −0.443, $p = 0.002$	———

CRM, CAD/CAM restorative material

Table 5
Results from the multivariate analysis of variance with Pillai's trace.

Independent Variable	Value	F	Hypothesis *df*	Error *df*	*p*	Partial Eta squared
Material	1.893	556.7	10	316	< 0.001	0.946
Weight difference	0.940	491.6	5	157	< 0.001	0.940
Cycle	0.043	1.4	5	157	0.222	0.043
Material × Weight difference	0.938	27.9	10	316	< 0.001	0.469
Material × Cycle	0.111	1.9	10	316	0.050	0.056
Weight difference × Cycle	0.037	1.2	5	157	0.305	0.037
Material × Weight difference × Cycle	0.129	2.2	10	316	0.019	0.064

p values < 0.05 designate significant differences

Table 6
Test of between-subjects effects for the fixed factor material on mechanical properties.

Dependent Variable	Sum of Squares	df	Mean of Squares	F ratio	p value	Partial Eta squared
FS	105298.6	2	52649.3	482.3	< 0.001	0.857
ME	3043636336.0	2	1521818168.0	15613.2	< 0.001	0.995
MR	1.4	2	0.7	41.0	< 0.001	0.338
MT	188.3	2	94.2	417.9	< 0.001	0.838
ER	48.1	2	24.0	578.6	< 0.001	0.878

p values < 0.05 designate significant differences.

Table 7
Test of between-subjects effects for the fixed factor weight difference on mechanical properties.

Dependent Variable	Sum of Squares	df	Mean of Squares	F ratio	p value	Partial Eta squared
FS	48231.5	1	48231.5	441.8	< 0.001	0.733
ME	57836002.8	1	57836002.8	593.4	< 0.001	0.787
MR	5.7	1	5.7	332.4	< 0.001	0.674
MT	1.9	1	1.9	8.6	0.004	0.050
ER	5.9	1	5.9	142.4	< 0.001	0.469

p values < 0.05 designate significant differences.

Table 8
Test of between-subjects effects for the fixed factor cycle of storage on mechanical properties.

Dependent Variable	Sum of Squares	df	Mean of Squares	F ratio	p value	Partial Eta squared
FS	323.9	1	323.9	2.967	0.087	0.018
ME	255772.0	1	255772.0	2.624	0.107	0.016
MR	0.001	1	0.001	0.039	0.844	0.000
MT	0.362	1	0.362	1.606	0.207	0.010
ER	0.075	1	0.075	1.816	0.180	0.011

p values < 0.05 designate significant differences.

always showed the significantly highest values of loss tangent with thermocycling and concurrently positive specimen weight differences, independent of the CRM investigated (Fig. 8) ($p < 0.001$). Conversely, for drying (negative weight differences and water desorption), the significantly lowest loss tangent data were repeatedly acquired (Fig. 8), while under the same conditions, the highest mechanical properties were concurrently obtained (Figs. 3 - 7).

3.4.3. Materials

A comparison of the three different CRMs was made. For MPM, the significantly lowest datasets regarding FS and ME and the highest results for LU with SB positioned in between ($p < 0.001$) (lower case letters Figs. 3 - 4) were obtained after drying. A similar outcome was obtained after thermocycling, except that for FS, datasets of SB and MPM were not distinguishable ($p > 0.05$) and both together were significantly lower

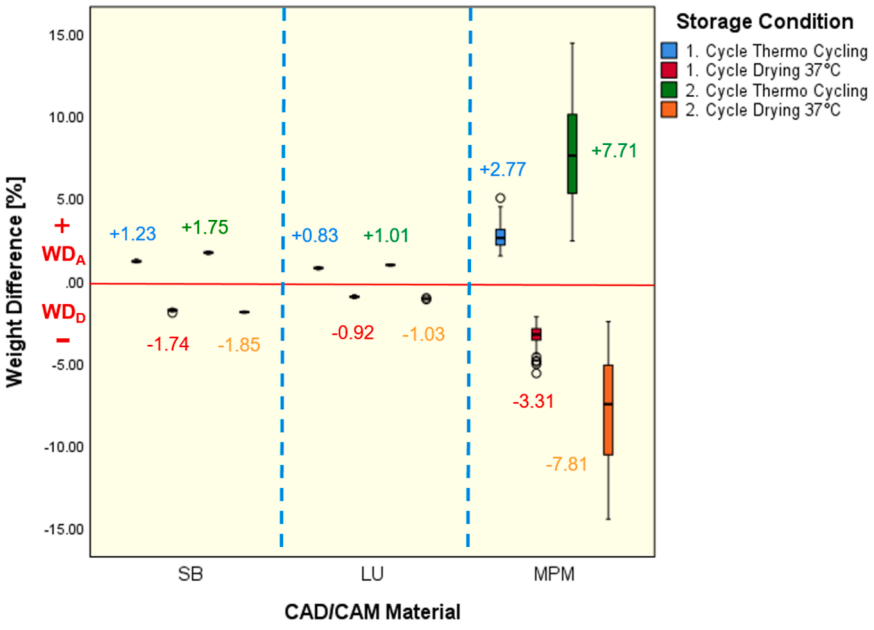

Fig. 2. Percentage weight differences between two different storage conditions. Missing identical uppercase letters on the top denote significant differences among cycles for the same CRM ($p < 0.05$). Missing identical lowercase letters below denote significant differences among different CRMs for the same cycles ($p < 0.05$). + WD_A, weight difference absorption; - WD_D, weight difference desorption; circles represent outliers.

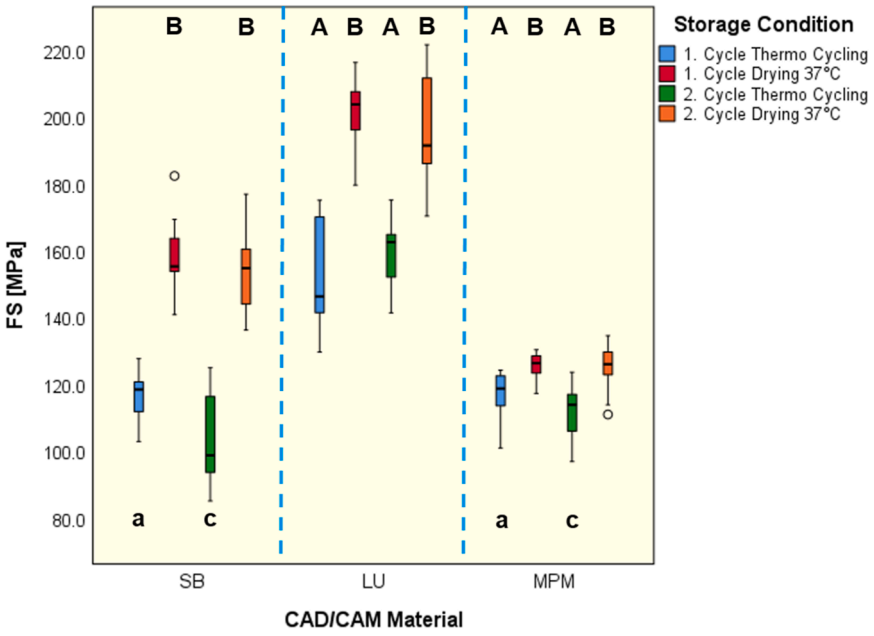

Fig. 3. FS datasets arranged according to CRMs and storage conditions. Identical uppercase letters on the top denote no significant difference among cycles for the same CRM ($p > 0.05$). Identical lowercase letters below denote no significant differences among different CRMs for the same cycles ($p > 0.05$). Circles represent outliers.

than the results of LU ($p < 0.001$) (lower case letters Fig. 3).

The situation changes when the datasets for MT (Fig. 6) and ER (Fig. 7), respectively, are compared. Now MPM always reveals the significantly highest results for both thermocycling and drying ($p < 0.001$), while SB and LU had the lowest results, which in most cases were not significantly different ($p > 0.05$). Concerning MR (lower case letters Fig. 5) the results for LU and MPM were not significantly different ($p > 0.05$), irrespective of whether thermocycling or drying data were evaluated. But the respective comparison with SB mostly revealed the significantly highest data sets for SB ($p < 0.05$) (lower case letters Fig. 5).

4. Discussion

4.1. Influence of storage condition on weight difference and water equilibrium

The well-known phenomenon that storage conditions may largely affect material characteristics and, ultimately, the long-term behavior of artificial restorative materials during their service life was also observed in this in vitro study. A perfect correlation between the storage condition and the sign of specimen weight differences was determined (χ^2 (1, $N = 450$) = 450,000, p < 0.001, $V = 1.0$). This indicates a well-defined

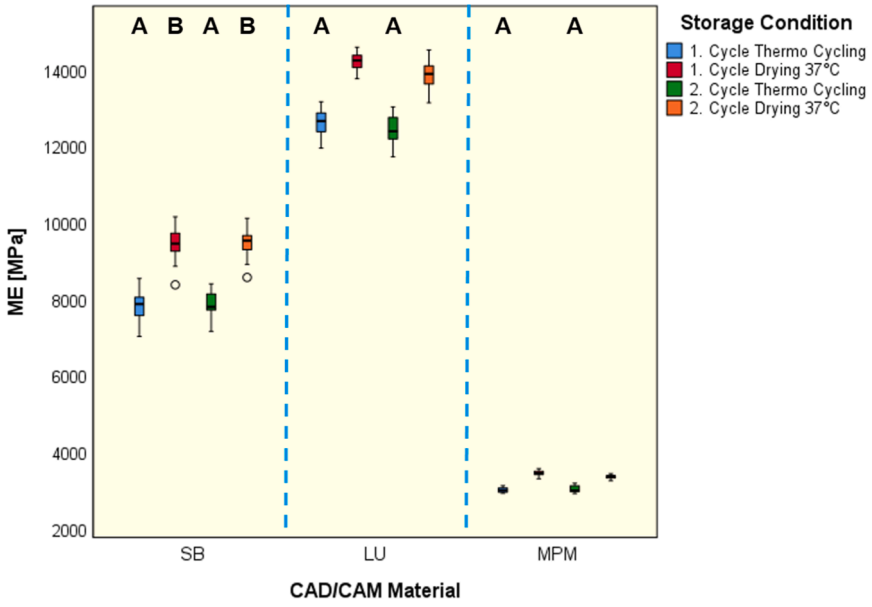

Fig. 4. ME datasets arranged according to CRMs and storage conditions. Identical uppercase letters on the top denote no significant difference among cycles for the same CRM ($p > 0.05$). Missing identical lowercase letters below denote significant differences among different CRMs for the same cycles ($p < 0.05$). Circles represent outliers.

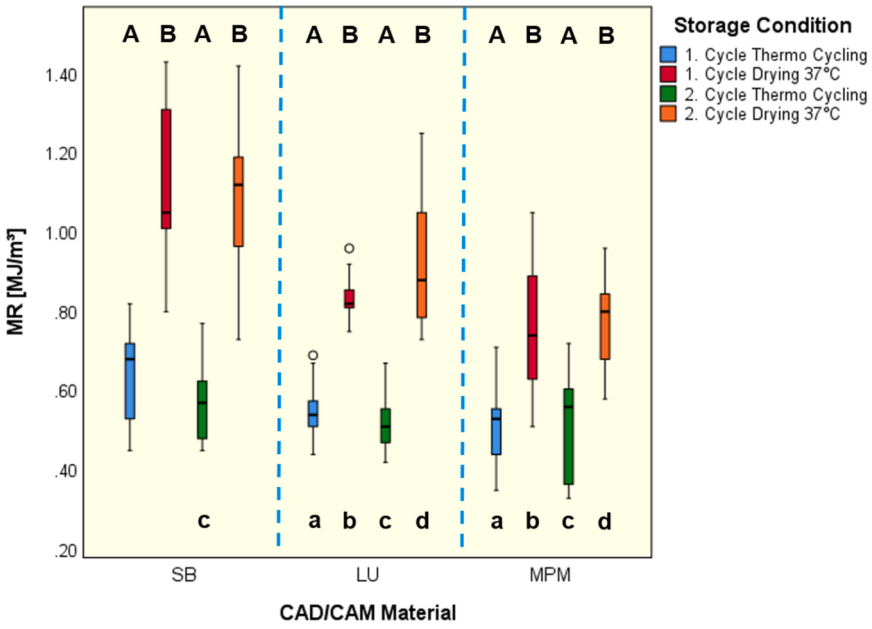

Fig. 5. MR datasets arranged according to CRMs and storage conditions. Identical uppercase letters on the top denote no significant difference among cycles for the same CRM ($p > 0.05$). Identical lowercase letters below denote no significant differences among different CRMs for the same cycles ($p > 0.05$). Circles represent outliers.

water absorption behavior of CRM specimens during thermocycling and likewise a specific desorption characteristic during the respective drying process. Therefore, the first null hypothesis that no correlation exists between the 'sign of the weight difference' and the 'storage condition' has to be rejected.

In daily practice, the amount of absorbed water in artificial restorative materials as well as in natural tissues may vary considerably. It strongly depends on the chemical composition, molecular structure, and hydrophilicity of the investigated material, especially in polymer-based restorative materials [11,62]. Various equilibrium states may therefore be assumed to exist under wet conditions. These appear to be latently present and have the potential to be specifically triggered and shifted to either higher or lower degrees of water content. Such effects seem to have been realized in the CRMs examined in this study, which indicates the presence of invertible processes. Lohbauer et al. also recently investigated the water uptake of different CRMs but for the first time via coulometric titration and they reported a 'base water content' that could modulate the amount of additional water sorption [63]. This observation seems to indicate the existence of alterable water equilibrium states, which may be influenced by exogenous factors that ultimately affect material properties and thus induce variable material behavior. Unfortunately, it is not clear whether the postulated 'base water content' (bound water) in the study of Lohbauer may be explicitly assigned to existing and separated 'water molecules' that could still be evaporated

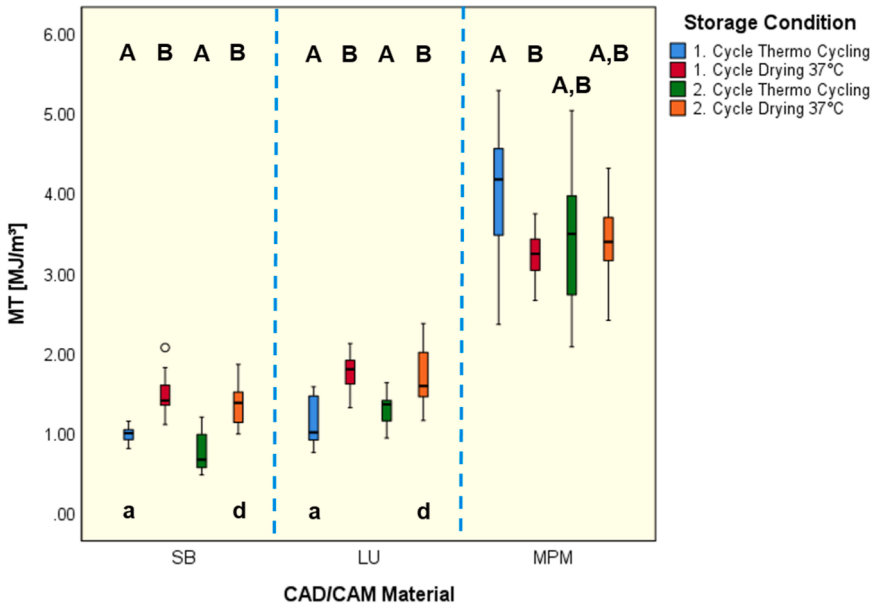

Fig. 6. MT datasets arranged according to CRMs and storage conditions. Identical uppercase letters on the top denote no significant difference among cycles for the same CRM ($p > 0.05$). Identical lowercase letters below denote no significant differences among different CRMs for the same cycles ($p > 0.05$). Circles represent outliers.

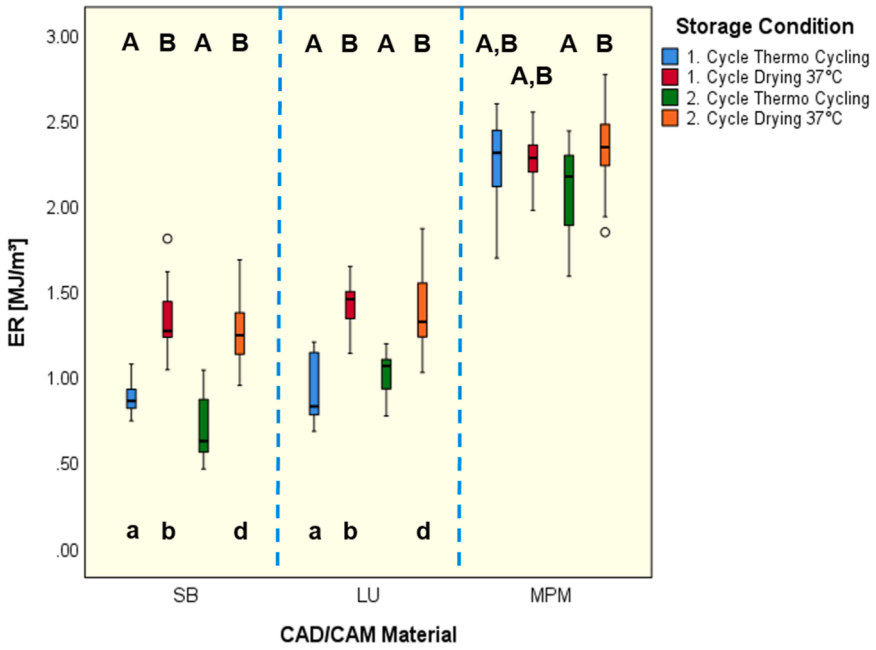

Fig. 7. ER datasets arranged according to CRMs and storage conditions. Identical uppercase letters on the top denote no significant difference among cycles for the same CRM ($p > 0.05$). Identical lowercase letters below denote no significant differences among different CRMs for the same cycles ($p > 0.05$). Circles represent outliers.

and quantified or to the 'free water' (unbound), now under much severer conditions. Or should this 'base water content' instead be related to chemical reaction processes (where water is released as a reaction by-product) taking place under the markedly high testing temperatures of 200 °C reported by Lohbauer. These conditions were obviously necessary to completely evaporate the water of CRMs in the respective study so that is was finally available for determination via coulometric titration [63]. Such water-releasing chemical reaction processes may involve well-known transformation processes on hygroscopic and uncoated hydroxylated filler particle surfaces (omnipresent equilibria) [64,65] or equally on the respective silane-coated surface structures, where continuing condensation processes and equilibria in the silane layer may constantly release water [26,66], especially at the markedly elevated temperatures of 200 °C described by Lohbauer [63].

The 'free volume theory' [67] explains in detail how solvents in glassy polymers diffuse depending on the motion capability of individual polymer chains. The main outcome of this theory is still a dual-mode model, which supposes that the amount of captured solvent or water molecules comprise two different populations in glassy polymers, namely those in the hole-free volume (space is continuously redistributed by thermal fluctuation and responsible for Henry's sorption) and those in the interstitial free volume (remaining space of pre-existing

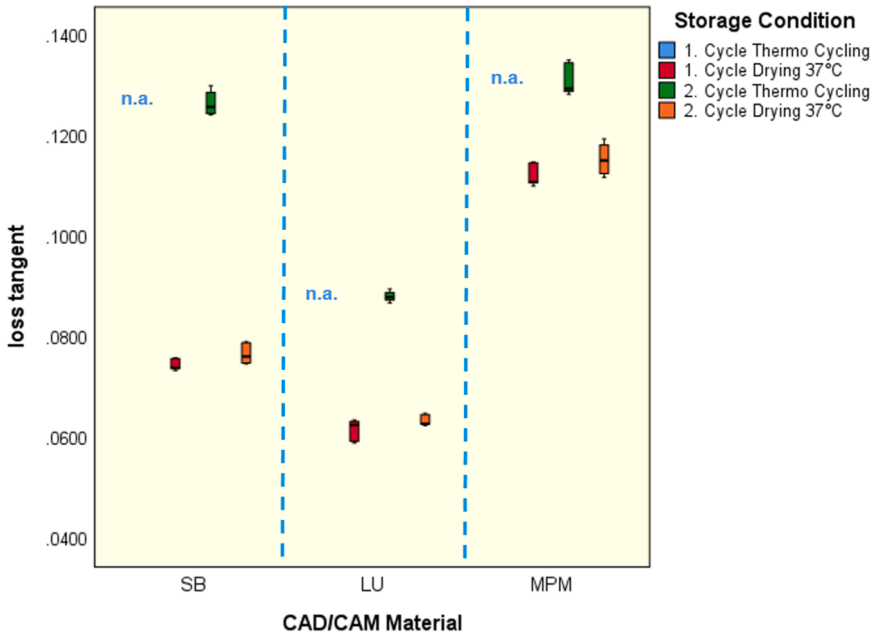

Fig. 8. Loss tangent values arranged according to CRMs and storage conditions. Missing identical uppercase letters on the top denote significant differences among cycles for the same CRM ($p < 0.05$). Missing identical lowercase letters below denote significant differences among different CRMs for the same cycles ($p < 0.05$). n. a., not available.

un-relaxed free volume responsible for Langmuir's sorption) [67,68]. To some extent, this dual-mode model interpretation may plausibly support the results and presumptions of Lohbauer et al. [63], and it also provides a better understanding of the equilibrium conditions observed throughout the water sorption and desorption processes in our study. Nevertheless, further investigations for a deeper understanding of such free-volume phenomena are needed for a more profound understanding of solvent motion and equilibria processes in dental polymers, composites, and especially the CRMs that are now more frequently used.

Furthermore, the question arises as to whether shifts of equilibrium states of the water content to an extreme side can be assigned to be reversible and whether they can be reverted to the original condition without leaving irreversibly destroyed structures behind [69,70]. Our study provides an initial answer for CRMs by demonstrating a reversibility of water sorption/desorption for two cycle times. For the composite-based materials (SB, LU) a very similar behavior is shown in the second storage cycle compared to the first (Fig. 2) (SB: 1. Cycle +1.23%; 2. Cycle +1.75%; LU: 1. Cycle +0.83%; 2. Cycle +1.01%). However, for the PMMA-based CRM (MPM) under the same conditions, a considerably higher effect of sorption (+7.71%) and desorption (−7.81%), together with rather high standard deviations, were observed in the second storage cycle compared to the first (+2.77%; −3.31%) (Fig. 2). This unexpected behavior of MPM compared to SB und LU may be explained via the assumption that during the first water storage (thermocycling) unreacted monomers and further freely movable components may have leached from the specimens while simultaneously leaving behind empty spaces inside the macromolecular structures into which additional water molecules could have penetrated later during the second storage cycle (thermocycling). This observation was also reported by Sideridou et al. [71], who investigated dimensional changes of light-cured dimethacrylate resins after sorption and desorption of water or ethanol in two independent treatment cycles. In the first cycle, they always found significantly higher SL(%) values (solubility of unreacted monomer) compared to the second storage cycle. At the same time, values of the calculated weight increase (percentage of weight increase of specimens - WI(%)) were always significantly higher in the second storage cycle. Unfortunately, no information concerning the impact of this phenomenon on mechanical properties is available for that study.

Our study revealed only a very weak correlation between the 'sign of the weight difference' and the 'cycle of storage' (χ^2 (1, $N = 450$) $= 3.571$, $p = 0.059$, $V = 0.089$). This implies that the observed effects on the behavior of CRMs during the respective sorption and desorption processes occur in a similar manner in each treatment cycle and therefore appear to be independent of the treatment cycle. A very similar outcome was also observed for the parameters investigated by Sideridou et al. [71] (percentage water sorption, volume increase, degree of swelling), which showed no significant differences between two separate treatment cycles irrespective of whether water or ethanol was used for the sorption and desorption process in cured resin blends. This perfectly corroborates our results.

4.2. *Influence of weight difference and water content on mechanical properties*

A significant effect of the independent variable 'weight difference' on the mechanical properties was observed, which simultaneously showed a large effect size ($p < 0.001$, $\eta_p^2 = 0.940$). Furthermore, very strong 'negative' linear relationships were observed between weight difference and mechanical properties but very strong 'positive' linear relationships were determined between weight difference and all loss tangent data. Therefore, the second null hypothesis that the mechanical properties of CAD/CAM restorative materials are independent of the sign of the weight difference has to be rejected.

The frequently described phenomenon that mutable solvent sorption and desorption processes in artificial dental restorative materials may markedly alter their material structures [72,73], dimensions [71,74,75], and hence likewise change their mechanical properties [76] during their service life was also observed in our study. Unfortunately, in some previous investigations, such changes due to extensive water uptake were prematurely attributed to persistent hydrolytic degradation processes [2–6] and consequently to long-term mechanical deterioration. On the other hand, many authors primarily associate water uptake more logically with swelling processes of polymer networks [1], which are particularly perceptible in altered material properties and consequently in diverging restoration behavior. Nevertheless, in most of these

investigations, very little, if any, information is available about whether the observed effects appear to be reversible or are associated with equilibrium processes, as demonstrated in our study. For the sake of simplicity, early studies investigated this effect more frequently for pure resin systems containing no reinforcing fillers. For example, the first results were reported for polymethylmethacrylate in 1952 during research on its viscoelastic material behavior [77]. In that study, water uptake markedly lowered the modulus data that were continuously recovered during a steadily increased oven storage time at 108 °C. The authors concluded 'It seems clear-cut that the change in modulus follows the water loss' demonstrating a continuous increase in modulus data [77]. Identical results were observed in our study for the congeneric polymethylmethacrylate-based MPM with the observed effects for ME even being repeatable a second time (Fig. 4). A very similar outcome was later reported for different methacrylate-based resin blends commonly used in dental composite materials [78] and related resin blends comparable with commercial bonding systems where the 'decrease in modulus was proportional to the degree of water sorption' [62]. Interestingly, this effect of modulus decimation was only observed after specimen storage in water and could not be substantiated with the same samples stored in a hydrophobic liquid like hexadecane [62]. This observation clearly shows that the solvent uptake and its resulting influence on long-term material properties strongly depends on the polarity of the solvent molecules being absorbed. Similar effects were previously reported for matrix and interfacial cracks that occurred in structures with absorbed ethanol as a solvent but which were not similarly detected in alternative water-based systems [16]. Further comparable effects were discovered for aromatic dimethacrylate resins and their fluorinated counterparts, which showed significantly less water sorption and thus decreased mechanical property degradation for the corresponding fluorinated resin matrix [79,80]. Generally, the closer the match between the polarities of solvent and substrate molecules, the greater the likelihood of solvent uptake together with the induced solvent-inherent influences on the glass transition temperature (T_g) of polymeric structures [40,81]. Hence, solvent molecules are considered to change the polymer microstructure. They are capable of migrating in between polymer chains during the swelling and plasticization process and hence loosening structures and facilitating chain movement and slipping phenomena [82], and in this way, ultimately lower the glass transition temperature (T_g). As a result, common mechanical properties may be considerably reduced because the stiffness and rigidity of structures are markedly degraded. This solvent-induced impact on material properties was similarly observed in our study for all CRMs investigated under wet conditions, and the observed effects were even reversible and repeatable. While FS, ME, and MR datasets, which primarily describe a material's stiffness and rigidity, were always significantly decreased after water uptake during the thermocycling process (Figs. 3 - 5), concurrently, loss tangent data, describing merely tough and damping material characteristics, showed markedly increased values (Fig. 8) at all times. Hence, this result explicitly exemplifies a gain in energy dissipation and damping properties of CRMs solely due to an increase in water content. A very similar effect, also resulting from a lowered glass transition temperature, induced a reduction in the storage modulus of dental nanofilled light-curing resin composites [18] while at the same time a significant increase in loss tangent values was observed. This result perfectly corroborates the findings of our study.

A further meaningful insight into water absorption effects and equilibrium states is gained if filler particles are added to a resin matrix. Söderholm et al. [70,83] reported 'a significant strength recovery after dehydration' during tensile testing when pooled datasets of different commercial composite specimens were compared after previous storage in distilled water (60 °C, 6 months). Initial pooled values of dry samples (42.2 MPa) were again closely approached (30.8 MPa) after drying (desiccator 60 °C, 2 weeks) when compared to the previously determined results of wet specimens (23.3 MPa). In the same study, data recovery for individual composite materials after the wetting and drying processes appeared to be strongly dependent on the filler composition and the filler surface treatment. While some composites showed a durable strength degradation without any data recovery, a few materials almost recovered or even exceeded their original values [70]. This observation for composite-based materials provides an early indication of the assumption that changes to mechanical properties, explicitly due to water sorption phenomena, may also be based on equilibrium effects of at least partly reversible processes, as already observed in just pure resin systems. Similarly, in our study, equilibrium processes during water sorption and desorption were detected for both composite-based CRMs (SB, LU) when mechanical properties were compared after repeated thermocycling or the respective drying processes. Irrespective of whether wet or dry conditions are considered, previous material properties were repeatedly attained and completely recovered even though a second independent cycle of specimen treatment was executed. Therefore, no signs of irreversible processes or material degradation were substantiated in any cases, which supports the assumption of harmless equilibrium processes being involved during regular water sorption in composite-based CRMs. However, the main difference between the results obtained in our study and those of the early composite investigations of Söderholm [70] can be attributed to the optimized silanization procedures [21,22] and modern drying techniques used in the meantime for filler coating and surface treatments. This may explain Söderholm's results for some composites, which did not even partly recover their properties after drying and where, consequently, severe filler degradation processes could still have occurred and played an important role [84]. Nevertheless, with today's sophisticated silane-based filler coating technology [81], water-induced property degradation in contemporary composite materials is apparently due more to the effects primarily emerging from resin and polymer structures, which may be particularly prone to a water-induced drop of their glass transition temperature (T_g) [85,86].

Despite this, in modern composite materials [87,88] and experimental composites [89], a steadily increasing amount of well-silanized fillers continuously reduces the percentage proportion of the resin matrix and hence also the water sorption capacity of the resulting restorative materials. A very similar effect was recently described for CRMs by Silikas et al. [87], who found a negative relationship between the filler weight percentage and the sorption capability of CRMs in water and artificial saliva. Consequently, with increased filler content, not just the water uptake is reduced but also potentially the well-known water--induced effect of mechanical property degradation. This coincidently emerges with the general phenomenon that an increased filler content fundamentally raises common mechanical properties [89–91]. This special effect of the filler was similarly observed in our study, where MPM exhibited the lowest filler percentage and LU the highest (Table 1). At the same time, MPM showed the highest water absorption (gain in weight after thermocycling) and LU the lowest water uptake with SB at all times in between (Fig. 2). The considerably high water uptake of SB compared to LU was also independently observed in recent studies [87, 92] and used in our previous publication to explain the rather high mechanical property decline for SB after thermocycling in comparison to LU and further investigated CRMs [45]. The same result was reproduced in the present study but with the main difference that the observed effect of property degradation for SB und LU following water sorption appeared to be completely reversible after drying the respective specimens, even if repeated treatment cycles were additionally applied. This finding clearly confirms the existence of invertible equilibrium processes during mutable water sorption of composite-based CRMs and so also verifies the presence of induced reversible effects on the alteration of mechanical properties.

In contrast to the results discussed above, where for all investigated CRMs, conventional mechanical properties invariably revealed a considerable but reversible degradation after water sorption, the energy dissipation and material damping effects, partially emerging via viscoelastic material behavior (loss tangent data) are inversely affected

(Fig. 8; Table 4) with a positive impact on material stability. This likewise reversible effect implies a considerable improvement of destructive energy attenuation in the wet condition for CRMs and contributes to protect restorations from premature failure. That may increase the service life, although during the respective water uptake, conventional mechanical properties, which mainly characterize a material's rigidity and stiffness, are concurrently degraded. A very similar effect was previously described for loss tangent data of 'luting materials' [10], 'nanofilled resin composites' [18], and further for 'posterior teeth composites' [76,93], where this effect exhibited a marked decrease of the modulus and strength data during water uptake but concomitantly demonstrated continuously increased creep properties, which have to be considered as a time-dependent damping effect too [94]. This inverse correlation of Young's modulus and loss tangent data has already been documented in detail by Ashby diagrams [95] and was recently used to explain different damping properties of CRMs [96]. At first glance, the apparently opposite effect of water uptake on the modulus and viscoelastic properties appears to be counterproductive to attain the overall aim of long-lasting restoration stability. However, this concept was developed by nature over millions of years and is realized in numerous natural composite materials to efficaciously protect biological structures like bones [34], teeth [97], and other tissues [98,99] from unwanted overload and its destructive impact. Hence, water sorption should not universally be viewed as a phenomenon that provokes irreversible detrimental effects on common mechanical properties of artificial restorative materials. Rather, like in natural composites, its emergence appears to be vitally important to reduce rigidity and brittleness, increase material flexibility and toughness, and consequently improve damping properties in artificial structures based on the model of nature. The presence of water is evidently crucial to achieving a suitable balance between all essential material properties with the aim of optimally replacing natural tissues with artificial restorative materials as biomimetically as possible to maximize the chances of a long-lasting service life. Ferracane et al. [100] also highlighted the importance of long-term water aging processes to reliably assess the stability of material properties in the wet condition. For their experimental materials, they concluded 'it is unlikely that dental composites will undergo drastic increases in wear or fracture rate as a result of degradation of the polymer matrix, filler, or filler-matrix interface in water' [100]. This perception is also confirmed by the results from our study for CRMs, which for water-based storage media show reversible and repeatable material property changes resulting from a mutable water content that obviously belongs to variable equilibrium states. Furthermore, varying water uptake seems to induce a positive effect on damping characteristics, crack behavior, and hence material stability. Complementary investigations to assess the influence of mutable water content on crack initiation and crack propagation are currently being performed in our labs.

The pronounced effect of water uptake on damping characteristics of CRMs is most obvious for SB in the present study because the gain of loss tangent data in this particular case was the highest observed (almost doubled) followed by LU and MPM (Fig. 8). Very similar results showing water-induced increases in creep properties and hence damping characteristics were previously reported by Ruyter et al. [93] for composite inlay materials and recently by Silikas et al. [101] who investigated the viscoelastic stability of CRMs. For all dry specimens tested, they always reported a significantly lower 'creep strain' and 'creep recovery' compared to those specimens stored for three months in water. In their study, SB datasets constantly demonstrated the significantly highest creep strain results, especially in comparison to LU, thus corroborating the outcome described above for loss tangent data in our study. Unfortunately, Silikas provided no information about whether the results obtained were also repeatable. Nevertheless, the different behavior of SB and LU may be explained by their varying water uptake capabilities. Even though SB demonstrated only a slightly higher water uptake than LU (Fig. 2) [87,92] the influence of this effect on the swelling phenomenon, molecular slipping characteristics, and thus induced lowering of the glass transition temperature of the polymer matrix appears to be strong enough to markedly increase the loss tangent data of SB, which are significantly higher than those of LU and also very closely approaching the prominent results of MPM (Fig. 8). This particular outcome demonstrates that comparatively low damping characteristics of an artificial composite material in the dry condition may be unequivocally raised to significantly higher values solely due to the absorption of pure water while at the same time reversibly sacrificing some small amounts of high-level mechanical properties like FS and ME and so also proportionally discarding material rigidity and brittleness. It is self-evident that such powerful effects may have a multitude of different causes on the molecular level, and in many cases, strongly depend on the particular material composition and polymer crosslinking structures as well as the solvent and solute properties. A very similar stabilization effect of water uptake was reported by Ferracane et al. [16], who found a significant increase in fracture toughness data for experimental composites after water aging for 14 months. The results obtained were explained by different filler/matrix interactions assuming partial filler/matrix de-bonding effects [16]. Hence, previous literature was cited where poorly bonded fillers were supposed to provide sites on their surfaces that facilitate enhanced energy dissipation effects by increasing the total energy needed to propagate a crack, and therewith, simultaneously raising K_{IC} values [102,103]. Very similar and repeatedly reversible effects during multiple water uptake were recently observed for supramolecular fibers showing drastic changes in the material structure and, with that, improved stress-strain behavior, damping characteristics and an alterable super contraction [104]. In this particular case, all mechanical properties, especially the contraction behavior, appeared to be systematically tunable according to the humidity level, providing the opportunity to fabricate biomimetic muscles for prosthetic limbs. Consequently, future developments in composite and CRM technology should likewise focus on similar material structures with water-tunable properties, currently often based on hydrogel chemistry under wet conditions [105], to incorporate improved viscoelastic material characteristics, energy dissipation capabilities, fracture resistance, and thus long-term durability into biomimetic artificial restorative materials.

4.3. Influence of material on mechanical properties

Another important result of our study is the substantiation of a significant effect of the independent variable 'material' on the mechanical properties where a large effect size was observed ($p < 0.001$, $\eta_p^2 = 0.946$). Hence, the third null hypothesis that the mechanical properties of CRMs are independent of the material has to be rejected. As previously reported for CRMs and their common mechanical properties like FS and ME [45], also in the present study, significantly higher datasets were obtained for LU compared to MPM, with SB values perfectly positioned in between (Figs. 3 – 4). This ranking may be reasonably explained by the various filler weight percentages of the respective CRMs (Table 1) determined in the present study using the well-established ashing in air technique having advantages over the acetone dissolution method in this particular case [47]. As previously demonstrated for experimental composites [89,90] and contemporary filling materials [91], where a continuously increased filler amount was unequivocally accounted for a marked increase in common mechanical properties, similarly LU with its comparatively high filler loading showed the highest datasets for FS and ME observed in this study.

A reversed sequence of the overall ranking for the same CRMs was found regarding material properties like MT (Fig. 6) and ER (Fig. 7), where datasets partially describe energy dissipation properties, such as permanent plastic material deformation and creep effects. Hence, in these cases, MPM constantly exhibited the significantly highest results when compared with SB and LU, which corroborates perfectly with our previously published findings [45,46]. The deviant behavior can

similarly be explained via the different filler content of the CRMs investigated (Table 1) and also by means of their various possibilities to form crosslinking structures between polymer chains. Hence, the comparatively high filler content of LU and SB, in combination with their polymer structures based solely on bis-methacrylate resins that predominantly generate extended crosslink densities during the polymerization process, impede polymer chain movement, slipping of molecular structures and, hence relaxation processes on the molecular level. These effects impart more rigid and less tough material properties to the final restoration. In contrast, MPM, with its exceptionally high content of mono-methacrylate resins and consequently lower crosslink densities in the cured polymer structures, together with its lack of reinforcing fillers, logically allows markedly improved movement of molecular chains that results in pronounced tough material behavior. Hence, MPM shows considerably higher viscoelastic material deformation than LU and SB, consequently increasing MT and ER datasets. Similarly, the same assumption of polymer chain slipping on the molecular level can be used to explain markedly higher viscoelastic damping capabilities of MPM when compared to those of the other CRMs. MPM always showed the significantly highest loss tangent data irrespective of whether dry or wet specimens were compared (Fig. 8). An identical ranking of loss tangent data, corroborating the results of the present study, was previously reported where the same CRMs were investigated but instead after storage in distilled water (24 h; 37 °C) [106].

Finally, a totally different order of CRMs was determined in this study for MR datasets that describe just the pure elastic behavior of a material where Hooke's law is valid and no plastic material deformation occurs until very near the proportional limit [46]. All CRMs showed a significant reduction of MR (yield strength) in the wet condition (Fig. 5). A very similar water-induced effect was observed in a previous study, showing a comparable reduction of the flexural strength at the proportional limit for moistened polymethylmethacrylate-based denture base materials [107], thus corroborating the results for MPM in our study. However, SB nearly always had significantly higher datasets than LU and MPM (Fig. 5). This effect of a higher elastic energy conversion for SB during the three-point bending test appeared to be more pronounced after specimens were dried and is conceivably due to a decreased polymer chain movement and a lowered slipping effect being caused by a reduced moisture content between adjacent polymer chain crosslinks, thus enhancing material stiffness and rigidity. Furthermore, high crosslink densities may generally impede polymer chain movement. This interpretation should be treated with caution, as no supporting experimental data of the respective crosslink densities are available yet for a reliable comparison.

4.4. Impact on clinical practice

Our study shows that although water uptake may markedly reduce common mechanical properties of CRMs, this effect reveals no permanent harmful or destructive impact on the composite material. Rather, it seems that this process can be repeatedly reversed several times with recovery of the previous material properties. Furthermore, water absorption also results in very beneficial damping characteristics, which could potentially improve material stability and survival rates by providing biomimetic energy dissipation processes. This kind of damping effect, in particular, may contribute to preventing artificial material structures from being irreversibly destroyed in the long term. Very similar phenomena where water uptake induces substantial material flexibility and so simultaneously provokes pronounced damping characteristics appear to be perfectly realized in natural composite structures like bone [34,108], tooth [35, 97, 109], and antler [110], with this effect primarily emerging via a pronounced viscoelastic material behavior [111–113]. Hence, future developments in artificial restorative materials should mainly focus on continuously improving viscoelastic material properties, which are often intensified under wet conditions [18, 113] with considerably enhanced damping effects like those demonstrated in our study. Consequently, contrary to common perception, water uptake should no longer solely be viewed as an unfavorable and adverse effect that primarily impedes long-term material survival by degrading conventional mechanical properties. Instead, water uptake should be regarded as a vital process for the genesis of precious damping properties in natural and artificial environments.

4.5. Limitations of our study

A first limitation is the usage of pure water as a solvent to imitate absorption and desorption processes in the oral environment, although artificial salvia [114] and other food-simulating liquids like ethanol-water mixtures [115] are more frequently utilized. It is well-known that individual dietary habits and changes may involve a multitude of different solvent mixtures in the mouth with different pH values and salt concentrations, which therefore induce situation-specific corrosion and degradation processes. However, it is still very difficult to simulate such particular conditions in vitro with standardized procedures [116]. Nevertheless, water is involved in many studies as an integral part of various mixtures and has therefore become a standard solvent in most in vitro studies. We therefore used pure water in our study to simplify the handling of the double-walled heating chamber during the DMA measurement and, far more importantly, to standardize and facilitate the specimen weighing process, because other ingredients in water, especially inorganic salts, could have separated on surface structures during water evaporation thereby negatively influencing the data acquisition. Furthermore, osmosis phenomena that also commonly arise on interfacial surface layers in contact with concentrated salt solutions like 'brine' are still not understood in detail. Therefore, we wanted to avoid such effects in our study.

The CRMs investigated in our study were polymerized with optimized and standardized industrial procedures. This resulted in a uniform material quality compared to standard composite restorative materials cured under clinical and sometimes humid conditions with different procedures (chemical or light activated). This might result in different degrees of monomer conversions, unreacted monomers, and crosslink densities than in vivo, and that could considerably affect a material's solvent absorption and monomer elution capability, resulting in a markedly different material behavior during fracture mechanical tests.

For reasons of simplicity, we used a static test procedure for the three-point bending test in our study, although dynamic test methods based on cyclic loading conditions exist that could yield substantially different outcomes for the resistance of a material structure to crack initiation and crack propagation. Further experiments concerning this are currently underway in our labs. At present, we cannot state whether the results obtained for CRMs in our study are universally valid and can also be found for other contemporary, composite-based, restorative materials. Further standardized experiments in this line of work are strongly recommended to acquire a deeper understanding of long-term material behavior of composite-based, artificial restorative materials in the wet environment.

5. Conclusions

Within the limitations of the present in vitro investigation, the following conclusions can be drawn for resin-based CAD/CAM restorative materials. Repeated thermocycling of the same test specimens was invariably accompanied by controlled water absorption and a concomitant induced loss of common mechanical properties while simultaneously bringing about markedly improved damping characteristics to dissipate detrimental fracture energy. Conversely, controlled drying of the same specimens recurrently increased mechanical properties by accurately converging measured values to the initial levels but concomitantly lowered damping characteristics and energy dissipation effects considerably. Despite repeated treatment of specimens under

different humid storage conditions and the resulting diverging water content, no evidence was found for persistent hydrolytic decomposition processes and, accordingly, long-term mechanical degradation of CRMs. Controlled water uptake in artificial restorative materials appears to balance, instead of permanently destroying, a multitude of material properties. It should therefore be considered vital for the development of pronounced damping effects in biomimetic restorative materials.

Declaration of Competing Interest

The authors declare that they have no known competing financial interests or personal relationships that could have appeared to influence the work reported in this paper.

Acknowledgements

The authors thank Dr. Johannes Herrmann for assistance with the statistical analysis. We gratefully recognize Mettler Toledo Giessen for providing a DMA 1 with customized lower support bars free of charge. The authors received no financial support and declare no potential conflicts of interest with respect to the authorship and/or publication of this article. This research did not receive any specific grant from funding agencies in the public, commercial, or not-for-profit sectors.

References

[1] Ferracane JL. Hygroscopic and hydrolytic effects in dental polymer networks. Dent Mater 2006;22(3):211–22. https://doi.org/10.1016/j.dental.2005.05.005.
[2] Wendler M, Stenger A, Ripper J, Priewich E, Belli R, Lohbauer U. Mechanical degradation of contemporary CAD/CAM resin composite materials after water ageing. Dent Mater 2021;37(7):1156–67. https://doi.org/10.1016/j.dental.2021.04.002.
[3] Lee C, Yamaguchi S, Imazato S. Quantitative evaluation of the degradation amount of the silane coupling layer of CAD/CAM resin composites by water absorption. J Prosthodont Res 2023;67(1):55–61. https://doi.org/10.2186/jpr.JPR_D_21_00236.
[4] Ilie N. Degradation of Dental Methacrylate-Based Composites in Simulated Clinical Immersion Media. J Funct Biomater 2022;13(1). https://doi.org/10.3390/jfb13010025.
[5] Sagsoz O, Polat Sagsoz N. Chemical degradation of dental CAD/CAM materials. Biomed Mater Eng 2019;30(4):419–26. https://doi.org/10.3233/BME-191063.
[6] Klauer E, Belli R, Petschelt A, Lohbauer U. Mechanical and hydrolytic degradation of an Ormocer®-based Bis-GMA-free resin composite. Clin Oral Investig 2019;23(5):2113–21. https://doi.org/10.1007/s00784-018-2651-3.
[7] Amaral FL, Colucci V, Palma-Dibb RG, Corona SA. Assessment of in vitro methods used to promote adhesive interface degradation: a critical review. J Esthet Restor Dent 2007;19(6):340–53. https://doi.org/10.1111/j.1708-8240.2007.00134.x.
[8] Frassetto A, Breschi L, Turco G, Marchesi G, Di Lenarda R, Tay FR, Pashley DH, Cadenaro M. Mechanisms of degradation of the hybrid layer in adhesive dentistry and therapeutic agents to improve bond durability–A literature review. Dent Mater 2016;32(2):e41–53. https://doi.org/10.1016/j.dental.2015.11.007.
[9] Guo X, Yu Y, Gao S, Zhang Z, Zhao H. Biodegradation of Dental Resin-Based Composite - A Potential Factor Affecting the Bonding Effect: A Narrative Review. Biomedicines 2022;10(9). https://doi.org/10.3390/biomedicines10092313.
[10] Ilie N. Comparative analysis of static and viscoelastic mechanical behavior of different luting material categories after aging. Mater (Basel) 2021;14(6). https://doi.org/10.3390/ma14061452.
[11] Sideridou I, Tserki V, Papanastasiou G. Study of water sorption, solubility and modulus of elasticity of light-cured dimethacrylate-based dental resins. Biomaterials 2003;24(4):655–65. https://doi.org/10.1016/S0142-9612(02)00380-0.
[12] Kalachandra S, Turner DT. Water sorption of polymethacrylate networks: Bis-GMA/TEGDM copolymers. J Biomed Mater Res 1987;21(3):329–38. https://doi.org/10.1002/jbm.820210306.
[13] Braden M, Davy KWM. Water absorption characteristics of some unfilled resins. Biomaterials 1986;7(6):474–5. https://doi.org/10.1016/0142-9612(86)90039-6.
[14] Söderholm K-JM, Mukherjee R, Longmate J. Filler Leachability of Composites Stored in Distilled Water or Artificial Saliva. J Dent Res 1996;75(9):1692–9. https://doi.org/10.1177/00220345960750091201.
[15] Söderholm KJ, Zigan M, Ragan M, Fischlschweiger W, Bergman M. Hydrolytic degradation of dental composites. J Dent Res 1984;63(10):1248–54. https://doi.org/10.1177/00220345840630101701.
[16] Ferracane JL, Marker VA. Solvent degradation and reduced fracture toughness in aged composites. J Dent Res 1992;71(1):13–9. https://doi.org/10.1177/00220345920710010101.
[17] Boussès Y, Brulat-Bouchard N, Bouchard PO, Tillier Y. A numerical, theoretical and experimental study of the effect of thermocycling on the matrix-filler interface of dental restorative materials. Dent Mater 2021;37(5):772–82. https://doi.org/10.1016/j.dental.2021.01.010.
[18] Vouvoudi EC, Sideridou ID. Dynamic mechanical properties of dental nanofilled light-cured resin composites: Effect of food-simulating liquids. J Mech Behav Biomed Mater 2012;10:87–96. https://doi.org/10.1016/j.jmbbm.2012.02.007.
[19] Söderholm K-JM, Shang S-W. Molecular Orientation of Silane at the Surface of Colloidal Silica. J Dent Res 1993;72(6):1050–4. https://doi.org/10.1177/00220345930720061001.
[20] Chen TM, Brauer GM. Solvent effects on bonding organo-silane to silica surfaces. J Dent Res 1982;61(12):1439–43. https://doi.org/10.1177/00220345820610121301.
[21] Matinlinna JP, Lung CYK, Tsoi JKH. Silane adhesion mechanism in dental applications and surface treatments: A review. Dent Mater 2018;34(1):13–28. https://doi.org/10.1016/j.dental.2017.09.002.
[22] Antonucci JM, Dickens SH, Fowler BO, Xu HH, McDonough WG. Chemistry of Silanes: Interfaces in Dental Polymers and Composites. J Res Natl Inst Stand Technol 2005;110(5):541–58. https://doi.org/10.6028/jres.110.081.
[23] Shah MB, Ferracane JL, Kruzic JJ. Mechanistic aspects of fatigue crack growth behavior in resin based dental restorative composites. Dent Mater 2009;25(7):909–16. https://doi.org/10.1016/j.dental.2009.01.097.
[24] Shah MB, Ferracane JL, Kruzic JJ. R-curve behavior and toughening mechanisms of resin-based dental composites: effects of hydration and post-cure heat treatment. Dent Mater 2009;25(6):760–70. https://doi.org/10.1016/j.dental.2008.12.004.
[25] Arikawa H, Kuwahata H, Seki H, Kanie T, Fujii K, Inoue K. Deterioration of mechanical properties of composite resins. Dent Mater J 1995;14(1):78–83. https://doi.org/10.4012/dmj.14.78.
[26] Plueddemann EP. Adhesion through silane coupling agents. J Adhes 1970;2:184–201. https://doi.org/10.1080/0021846708544592.
[27] Sideridou ID, Karabela MM. Effect of the amount of 3-methacyloxypropyltrimethoxysilane coupling agent on physical properties of dental resin nanocomposites. Dent Mater 2009;25(11):1315–24. https://doi.org/10.1016/j.dental.2009.03.016.
[28] Ezazi M, Ye Q, Misra A, Tamerler C, Spencer P. Autonomous-Strengthening Adhesive Provides Hydrolysis-Resistance and Enhanced Mechanical Properties in Wet Conditions. Molecules 2022;27(17). https://doi.org/10.3390/molecules27175505.
[29] Huang W, Shishehbor M, Guarín-Zapata N, Kirchhofer ND, Li J, Cruz L, Wang T, Bhowmick S, Stauffer D, Manimunda P, Bozhilov KN, Caldwell R, Zavattieri P, Kisailus D. A natural impact-resistant bicontinuous composite nanoparticle coating. Nat Mater 2020;19(11):1236–43. https://doi.org/10.1038/s41563-020-0768-7.
[30] Fantner GE, Hassenkam T, Kindt JH, Weaver JC, Birkedal H, Pechenik L, Cutroni JA, Cidade GA, Stucky GD, Morse DE, Hansma PK. Sacrificial bonds and hidden length dissipate energy as mineralized fibrils separate during bone fracture. Nat Mater 2005;4(8):612–6. https://doi.org/10.1038/nmat1428.
[31] Fantner GE, Oroudjev E, Schitter G, Golde LS, Thurner P, Finch MM, Turner P, Gutsmann T, Morse DE, Hansma H, Hansma PK. Sacrificial bonds and hidden length: unraveling molecular mesostructures in tough materials. Biophys J 2006;90(4):1411–8. https://doi.org/10.1529/biophysj.105.069344.
[32] Truong MY, Dutta NK, Choudhury NR, Kim M, Elvin CM, Nairn KM, Hill AJ. The effect of hydration on molecular chain mobility and the viscoelastic behavior of resilin-mimetic protein-based hydrogels. Biomaterials 2011;32(33):8462–73. https://doi.org/10.1016/j.biomaterials.2011.07.064.
[33] Tadayon M, Amini S, Wang Z, Miserez A. Biomechanical Design of the Mantis Shrimp Saddle: A Biomineralized Spring Used for Rapid Raptorial Strikes. iScience 2018;8:271–82. https://doi.org/10.1016/j.isci.2018.08.022.
[34] Yan J, Daga A, Kumar R, Mecholsky JJ. Fracture toughness and work of fracture of hydrated, dehydrated, and ashed bovine bone. J Biomech 2008;41(9):1929–36. https://doi.org/10.1016/j.jbiomech.2008.03.037.
[35] Kruzic JJ, Nalla RK, Kinney JH, Ritchie RO. Crack blunting, crack bridging and resistance-curve fracture mechanics in dentin: effect of hydration. Biomaterials 2003;24(28):5209–21. https://doi.org/10.1016/s0142-9612(03)00458-7.
[36] Jameson MW, Hood JA, Tidmarsh BG. The effects of dehydration and rehydration on some mechanical properties of human dentine. J Biomech 1993;26(9):1055–65. https://doi.org/10.1016/s0021-9290(05)80005-3.
[37] Morresi AL, D'Amario M, Capogreco M, Gatto R, Marzo G, D'Arcangelo C, Monaco A. Thermal cycling for restorative materials: Does a standardized protocol exist in laboratory testing? A literature review. J Mech Behav Biomed Mater 2014;29:295–308. https://doi.org/10.1016/j.jmbbm.2013.09.013.
[38] Connelly RW, McCoy NR, Koros WJ, Hopfenberg HB, Stewart ME. The effect of sorbed penetrants on the aging of previously dilated glassy polymer powders. I. Lower alcohol and water sorption in poly(methyl methacrylate). J Appl Polym Sci 1987;34(2):703–19. https://doi.org/10.1002/app.1987.070340223.
[39] Alrahlah A, Silikas N, Watts DC. Hygroscopic expansion kinetics of dental resin-composites. Dent Mater 2014;30(2):143–8. https://doi.org/10.1016/j.dental.2013.10.010.
[40] Frisch HL. Sorption and transport in glassy polymers–a review. Polym Eng Sci 1980;20(1):2–13. https://doi.org/10.1002/pen.760200103.
[41] Cock DJ, Watts DC. Time-dependent Deformation of Composite Restorative Materials in Compression. J Dent Res 1985;64(2):147–50. https://doi.org/10.1177/00220345850640021101.
[42] Vaidyanathan J, Vaidyanathan TK. Flexural creep deformation and recovery in dental composites. J Dent 2001;29(8):545–51. https://doi.org/10.1016/S0300-5712(01)00049-5.

[43] Xu Y, Kim C-S, Saylor DM, Koo D. Polymer degradation and drug delivery in PLGA-based drug–polymer applications: A review of experiments and theories. J Biomed Mater Res - B Appl Biomater 2017;105(6):1692–716. https://doi.org/10.1002/jbm.b.33648.

[44] Joseph B, George A, Gopi S, Kalarikkal N, Thomas S. Polymer sutures for simultaneous wound healing and drug delivery - A review. Int J Pharm 2017;524(1-2):454–66. https://doi.org/10.1016/j.ijpharm.2017.03.041.

[45] Niem T, Youssef N, Wostmann B. Influence of accelerated ageing on the physical properties of CAD/CAM restorative materials. Clin Oral Investig 2019;24(7):2415–25. https://doi.org/10.1007/s00784-019-03101-w.

[46] Niem T, Youssef N, Wöstmann B. Energy dissipation capacities of CAD-CAM restorative materials: A comparative evaluation of resilience and toughness. J Prosthet Dent 2019;121(1):101–9. https://doi.org/10.1016/j.prosdent.2018.05.003.

[47] Salazar D, Dennison J, Yaman P. Inorganic and Prepolymerized Filler Analysis of Four Resin Composites. Oper Dent 2013;38(6):E201–9. https://doi.org/10.2341/12-474-l.

[48] Alamoush RA, Silikas N, Salim NA, Al-Nasrawi S, Satterthwaite JD. Effect of the Composition of CAD/CAM Composite Blocks on Mechanical Properties. Biomed Res Int 2018;2018:4893143. https://doi.org/10.1155/2018/4893143.

[49] ISO 6872. Dentistry - Ceramic Materials. Geneva, Switzerland: International Organization for Standardization; 2015.

[50] ASTM D790-15e2. Standard Test Methods for Flexural Properties of Unreinforced and Reinforced Plastics and Electrical Insulating Materials. West Conshohocken, PA: ASTM International; 2015.

[51] Daemi H, Rajabi-Zeleti S, Sardon H, Barikani M, Khademhosseini A, Baharvand H. A robust super-tough biodegradable elastomer engineered by supramolecular ionic interactions. Biomaterials 2016;84:54–63. https://doi.org/10.1016/j.biomaterials.2016.01.025.

[52] Prakki A, Cilli R, Vieira IM, Dudumas K, Pereira JC. Water sorption of CH3- and CF3-Bis-GMA based resins with additives. J Appl Oral Sci 2012;20(4):472–7. https://doi.org/10.1590/s1678-77572012000400014.

[53] ISO 9513. Metallic Materials - Calibration of Extensometer Systems Used in Uniaxial Testing. Geneva, Switzerland: International Organization for Standardization; 2013.

[54] Kaizer MR, Almeida JR, Goncalves APR, Zhang Y, Cava SS, Moraes RR. Silica Coating of Nonsilicate Nanoparticles for Resin-Based Composite Materials. J Dent Res 2016;95(12):1394–400. https://doi.org/10.1177/0022034516662022.

[55] Paphangkorakit J, Kanpittaya K, Pawanja N, Pitiphat W. Effect of chewing rate on meal intake. Eur J Oral Sci 2019;127(1):40–4. https://doi.org/10.1111/eos.12583.

[56] Bates JF, Stafford GD, Harrison A. Masticatory function - a review of the literature. III. Masticatory performance and efficiency. J Oral Rehabil 1976;3(1):57–67. https://doi.org/10.1111/j.1365-2842.1976.tb00929.x.

[57] White AK, Venn B, Lu LW, Rush E, Gallo LM, Yong JL, Farella M. A comparison of chewing rate between overweight and normal BMI individuals. Physiol Behav 2015;145:8–13. https://doi.org/10.1016/j.physbeh.2015.03.028.

[58] Po JM, Kieser JA, Gallo LM, Tésenyi AJ, Herbison P, Farella M. Time-frequency analysis of chewing activity in the natural environment. J Dent Res 2011;90(10):1206–10. https://doi.org/10.1177/0022034511416669.

[59] K.P. Menard, N.R. Menard, Dynamic Mechanical Analysis, 3rd ed., CRC Press, Abingdon, 2020.

[60] McHugh ML. The chi-square test of independence. Biochem Med 2013;23(2):143–9. https://doi.org/10.11613/bm.2013.018.

[61] Sullivan GM, Feinn R. Using effect size-or why the p value is not enough. J Grad Med Educ 2012;4(3):279–82. https://doi.org/10.4300/jgme-d-12-00156.1.

[62] Ito S, Hashimoto M, Wadgaonkar B, Svizero N, Carvalho RM, Yiu C, Rueggeberg FA, Foulger S, Saito T, Nishitani Y, Yoshiyama M, Tay FR, Pashley DH. Effects of resin hydrophilicity on water sorption and changes in modulus of elasticity. Biomaterials 2005;26(33):6449–59. https://doi.org/10.1016/j.biomaterials.2005.04.052.

[63] Faria ESAL, Heckel L, Belli R, Lohbauer U. Coulometric titration of water content and uptake in CAD/CAM chairside composites. Dent Mater 2022;38(5):789–96. https://doi.org/10.1016/j.dental.2022.04.012.

[64] Dalstein L, Potapova E, Tyrode E. The elusive silica/water interface: isolated silanols under water as revealed by vibrational sum frequency spectroscopy. Phys Chem Chem Phys 2017;19(16):10343–9. https://doi.org/10.1039/C7CP01507K.

[65] Bistafa C, Surblys D, Kusudo H, Yamaguchi Y. Water on hydroxylated silica surfaces: Work of adhesion, interfacial entropy, and droplet wetting. J Chem Phys 2021;155(6). https://doi.org/10.1063/5.0056718.

[66] Ishida H, Miller JD. Substrate effects on the chemisorbed and physisorbed layers of methacryl silane-modified particulate minerals. Macromolecules 1984;17(9):1659–66. https://doi.org/10.1021/ma00139a004.

[67] Ramesh N, Davis PK, Zielinski JM, Danner RP, Duda JL. Application of free-volume theory to self diffusion of solvents in polymers below the glass transition temperature: A review. J Polym Sci B: Polym Phys 2011;49(23):1629–44. https://doi.org/10.1002/polb.22366.

[68] Zielinski JM, Duda JL. Predicting polymer/solvent diffusion coefficients using free-volume theory. AICHE J 1992;38(3):405–15. https://doi.org/10.1002/aic.690380309.

[69] Braden M, Causton EE, Clarke RL. Diffusion of Water in Composite Filling Materials. J Dent Res 1976;55(5):730–2. https://doi.org/10.1177/00220345760550050501.

[70] Söderholm K-JM, Roberts MJ. Influence of water exposure on the tensile strength of composites. J Dent Res 1990;69(12):1812–6. https://doi.org/10.1177/00220345900690120501.

[71] Sideridou ID, Karabela MM, Vouvoudi E. Volumetric dimensional changes of dental light-cured dimethacrylate resins after sorption of water or ethanol. Dent Mater 2008;24(8):1131–6. https://doi.org/10.1016/j.dental.2007.12.009.

[72] Wei YJ, Chen YY, Jiang QS. Long-term hygroscopic dimensional changes of core buildup materials in deionized water and artificial saliva. Dent Mater J 2021;40(1):143–9. https://doi.org/10.4012/dmj.2019-340.

[73] Park JW, Ferracane JL. Water aging reverses residual stresses in hydrophilic dental composites. J Dent Res 2014;93(2):195–200. https://doi.org/10.1177/0022034513513905.

[74] McCabe JF, Rusby S. Water absorption, dimensional change and radial pressure in resin matrix dental restorative materials. Biomaterials 2004;25(18):4001–7. https://doi.org/10.1016/j.biomaterials.2003.10.088.

[75] Martin N, Jedynakiewicz NM, Fisher AC. Hygroscopic expansion and solubility of composite restoratives. Dent Mater 2003;19(2):77–86. https://doi.org/10.1016/S0109-5641(02)00015-5.

[76] Øysæd H, Ruyter IE. Composites for use in posterior teeth: Mechanical properties tested under dry and wet conditions. J Biomed Mater Res 1986;20(2):261–71. https://doi.org/10.1002/jbm.820200214.

[77] McLoughlin JR, Tobolsky AV. The viscoelastic behavior of polymethyl methacrylate. J Colloid Sci 1952;7(6):555–68. https://doi.org/10.1016/0095-8522(52)90039-1.

[78] Beatty MW, Swartz ML, Moore BK, Phillips RW, Roberts TA. Effect of crosslinking agent content, monomer functionality, and repeat unit chemistry on properties of unfilled resins. J Biomed Mater Res 1993;27(3):403–13. https://doi.org/10.1002/jbm.820270314.

[79] Tanaka J, Inoue K, Masamura H, Matsumura K, Nakai H, Inoue K. The Application of Fluorinated Aromatic Dimethacrylates to Experimental Light-cured Radiopaque Composite Resin, Containing Barium-Borosilicate Glass Filler - A Progress in Nonwaterdegradable Properties -, Dent. Mater J 1993;12(1):1–11. https://doi.org/10.4012/dmj.12.1.

[80] Srivastava R, Wolska J, Walkowiak-Kulikowska J, Koroniak H, Sun Y. Fluorinated bis-GMA as potential monomers for dental restorative composite materials. Eur Polym J 2017;90:334–43. https://doi.org/10.1016/j.eurpolymj.2017.03.027.

[81] Karmaker A, Prasad A, Sarkar NK. Characterization of adsorbed silane on fillers used in dental composite restoratives and its effect on composite properties. J Mater Sci Mater Med 2007;18(6):1157–62. https://doi.org/10.1007/s10856-007-0145-y.

[82] Wang B-G, Yamaguchi T, Nakao S-I. Solvent diffusion in amorphous glassy polymers. J Polym Sci B: Polym Phys 2000;38(6):846–56. https://doi.org/10.1002/(SICI)1099-0488(20000315)38:6.

[83] Söderholm KJ, Roberts MJ. Influence of water exposure on failure mechanisms of composite resins. No. 1296 J Dent Res 1989;68(1 suppl). https://doi.org/10.1177/00220345890680s102.

[84] Söderholm KJ. Degradation of glass filler in experimental composites. J Dent Res 1981;60(11):1867–75. https://doi.org/10.1177/00220345810600110701.

[85] Smith LSA, Schmitz V. The effect of water on the glass transition temperature of poly(methyl methacrylate). Polymer 1988;29(10):1871–8. https://doi.org/10.1016/0032-3861(88)90405-3.

[86] Hancock BC, Zografi G. The Relationship Between the Glass Transition Temperature and the Water Content of Amorphous Pharmaceutical Solids. Pharm Res 1994;11(4):471–7. https://doi.org/10.1023/A:1018941810744.

[87] Alamoush RA, Salim NA, Silikas N, Satterthwaite JD. Long-term hydrolytic stability of CAD/CAM composite blocks. Eur J Oral Sci 2022;130(1):e12834. https://doi.org/10.1111/eos.12834.

[88] Gornig DC, Maletz R, Ottl P, Warkentin M. Influence of artificial aging: mechanical and physicochemical properties of dental composites under static and dynamic compression. Clin Oral Investig 2022;26(2):1491–504. https://doi.org/10.1007/s00784-021-04122-0.

[89] Li Y, Swartz ML, Phillips RW, Moore BK, Roberts TA. Effect of filler content and size on properties of composites. J Dent Res 1985;64(12):1396–401. https://doi.org/10.1177/00220345850640121501.

[90] Tanimoto Y, Nishiwaki T, Nemoto K, Ben G. Effect of filler content on bending properties of dental composites: numerical simulation with the use of the finite-element method. J Biomed Mater Res 2004;71(1):188–95. https://doi.org/10.1002/jbm.b.30079.

[91] Kim KH, Ong JL, Okuno O. The effect of filler loading and morphology on the mechanical properties of contemporary composites. J Prosthet Dent 2002;87(6):642–9. https://doi.org/10.1067/mpr.2002.125179.

[92] Lauvahutanon S, Shiozawa M, Takahashi H, Iwasaki N, Oki M, Finger WJ, Arksornnukit M. Discoloration of various CAD/CAM blocks after immersion in coffee. Restor Dent Endod 2017;42(1):9–18. https://doi.org/10.5395/rde.2017.42.1.9.

[93] Kildal KK, Ruyter IE. How different curing methods affect mechanical properties of composites for inlays when tested in dry and wet conditions. Eur J Oral Sci 1997;105(4):353–61. https://doi.org/10.1111/j.1600-0722.1997.tb00252.x.

[94] Lazan BJ. Damping of Materials and Members in Structural Mechanics. Oxford: Pergamon Press; 1966.

[95] Ashby MF. Materials Selection in Mechanical Design. Oxford, United Kingdom: Elsevier Science & Technology; 1999.

[96] Niem T, Gonschorek S, Wostmann B. Investigation of the Damping Capabilities of Different Resin-Based CAD/CAM Restorative Materials. Polymers 2022;14(3):493. https://doi.org/10.3390/polym14030493.

[97] Kahler B, Swain MV, Moule A. Fracture-toughening mechanisms responsible for differences in work to fracture of hydrated and dehydrated dentine. J Biomech 2003;36(2):229–37. https://doi.org/10.1016/s0021-9290(02)00327-5.

[98] Dabrowska S, Grabowski K, Mlyniec A. Rehydration of the Tendon Fascicle Bundles Using Simulated Body Fluid Ensures Stable Mechanical Properties of the Samples. Mater (Basel) 2022;15(9). https://doi.org/10.3390/ma15093033.
[99] Ohshima H, Tsuji H, Hirano N, Ishihara H, Katoh Y, Yamada H. Water diffusion pathway, swelling pressure, and biomechanical properties of the intervertebral disc during compression load. Spine 1989;14(11):1234–44. https://doi.org/10.1097/00007632-198911000-00017.
[100] Ferracane JL, Berge HX, Condon JR. In vitro aging of dental composites in water-effect of degree of conversion, filler volume, and filler/matrix coupling. J Biomed Mater Res 1998;42(3):465–72. https://doi.org/10.1002/(sici)1097-4636(19981205)42:3.
[101] Alamoush RA, Satterthwaite JD, Silikas N, Watts DC. Viscoelastic stability of pre-cured resin-composite CAD/CAM structures. Dent Mater 2019;35(8):1166–72. https://doi.org/10.1016/j.dental.2019.05.007.
[102] Broutman LJ, Sahu S. The effect of interfacial bonding on the toughness of glass filled polymers. Mater Sci Eng 1971;8(2):98–107. https://doi.org/10.1016/0025-5416(71)90087-5.
[103] Ferracane JL. Fracture toughness of experimental dental composites. Trans 3rd World Biomater Congr 1988. pp. Abstr. No. 4B1-22.
[104] Wu Y, Shah DU, Wang B, Liu J, Ren X, Ramage MH, Scherman OA. Biomimetic Supramolecular Fibers Exhibit Water-Induced Supercontraction. Adv Mater 2018;30(27):1707169. https://doi.org/10.1002/adma.201707169.
[105] Rad IY, Lewis S, Barros MD, Kipper M, Stansbury JW. Suppression of hydrolytic degradation in labile polymer networks via integrated styrenic nanogels. Dent Mater 2021;37(8):1295–306. https://doi.org/10.1016/j.dental.2021.05.001.
[106] Niem T, Gonschorek S, Wostmann B. Evaluation of the damping capacity of common CAD/CAM restorative materials. J Mech Behav Biomed Mater 2022;126:104987. https://doi.org/10.1016/j.jmbbm.2021.104987.
[107] Takahashi Y, Chai J, Kawaguchi M. Effect of Water Sorption on the Resistance to Plastic Deformation of a Denture Base Material Relined With Four Different Denture Reline Materials. Int J Prosthodont 1998;11(1):49–54.
[108] Nyman JS, Roy A, Shen X, Acuna RL, Tyler JH, Wang X. The influence of water removal on the strength and toughness of cortical bone. J Biomech 2006;39(5):931–8. https://doi.org/10.1016/j.jbiomech.2005.01.012.
[109] Koldehoff J, Swain MV, Schneider GA. Influence of water and protein content on the creep behavior in dental enamel. Acta Biomater 2023;158:393–411. https://doi.org/10.1016/j.actbio.2023.01.018.
[110] Chen X, Qian T, Hang F, Chen X. Water promotes the formation of fibril bridging in antler bone illuminated by in situ AFM testing. J Mech Behav Biomed Mater 2021;120:104580. https://doi.org/10.1016/j.jmbbm.2021.104580.
[111] Yi Q, Feng X, Zhang C, Wang X, Wu X, Wang J, Cui F, Wang S. Comparison of dynamic mechanical properties of dentin between deciduous and permanent teeth. Connect Tissue Res 2021;62(4):402–10. https://doi.org/10.1080/03008207.2020.1758684.
[112] Emamian A, Aghajani F, Safshekan F, Tafazzoli-Shadpour M. Nonlinear viscoelastic properties of human dentin under uniaxial tension. Dent Mater 2021;37(2):e59–68. https://doi.org/10.1016/j.dental.2020.10.025.
[113] Cisneros T, Zaytsev D, Seyedkavoosi S, Panfilov P, Gutkin MY, Sevostianov I. Effect of saturation on the viscoelastic properties of dentin. J Mech Behav Biomed Mater 2021;114:104143. https://doi.org/10.1016/j.jmbbm.2020.104143.
[114] Gal JY, Fovet Y, Adib-Yadzi M. About a synthetic saliva for in vitro studies. Talanta 2001;53(6):1103–15. https://doi.org/10.1016/s0039-9140(00)00618-4.
[115] McKinney JE, Wu W. Chemical softening and wear of dental composites. J Dent Res 1985;64(11):1326–31. https://doi.org/10.1177/00220345850640111601.
[116] Musanje L, Darvell BW. Aspects of water sorption from the air, water and artificial saliva in resin composite restorative materials. Dent Mater 2003;19(5):414–22. https://doi.org/10.1016/s0109-5641(02)00085-4.